A *coumaroyl-ester-3-hydroxylase* Insertion Mutant Reveals the Existence of Nonredundant *meta*-Hydroxylation Pathways and Essential Roles for Phenolic Precursors in Cell Expansion and Plant Growth[1][W][OA]

Nawroz Abdulrazzak, Brigitte Pollet, Jürgen Ehlting, Kim Larsen, Carole Asnaghi, Sebastien Ronseau, Caroline Proux, Mathieu Erhardt, Virginie Seltzer, Jean-Pierre Renou, Pascaline Ullmann, Markus Pauly, Catherine Lapierre, and Danièle Werck-Reichhart*

Department of Plant Metabolic Responses (N.A., J.E., C.A., S.R., P.U., D.W.-R.) and Department Cell Biology (M.E., V.S.), Institute of Plant Molecular Biology Centre National de la Recherche Scientifique-Unité Propre de Recherche 2357, Université Louis Pasteur, 67000 Strasbourg, France; Laboratoire de Chimie Biologique-Unité Mixte de Recherche 206, Institut National de la Recherche Agronomique-Institut National Agronomique Paris-Grignon, 78850 Thiverval-Grignon, France (B.P., C.L.); Plant Cell Wall Group, Max Planck Institute for Molecular Plant Physiology, 14476 Golm, Germany (K.L., M.P.); and Unité de Recherche Génomique Végétale, 91057 Evry cedex, France (C.P., J.-P.R.)

Cytochromes P450 monooxygenases from the CYP98 family catalyze the *meta*-hydroxylation step in the phenylpropanoid biosynthetic pathway. The *ref8* Arabidopsis (*Arabidopsis thaliana*) mutant, with a point mutation in the *CYP98A3* gene, was previously described to show developmental defects, changes in lignin composition, and lack of soluble sinapoyl esters. We isolated a T-DNA insertion mutant in *CYP98A3* and show that this mutation leads to a more drastic inhibition of plant development and inhibition of cell growth. Similar to the *ref8* mutant, the insertion mutant has reduced lignin content, with stem lignin essentially made of *p*-hydroxyphenyl units and trace amounts of guaiacyl and syringyl units. However, its roots display an ectopic lignification and a substantial proportion of guaiacyl and syringyl units, suggesting the occurrence of an alternative CYP98A3-independent *meta*-hydroxylation mechanism active mainly in the roots. Relative to the control, mutant plantlets produce very low amounts of sinapoyl esters, but accumulate flavonol glycosides. Reduced cell growth seems correlated with alterations in the abundance of cell wall polysaccharides, in particular decrease in crystalline cellulose, and profound modifications in gene expression and homeostasis reminiscent of a stress response. CYP98A3 thus constitutes a critical bottleneck in the phenylpropanoid pathway and in the synthesis of compounds controlling plant development. *CYP98A3* cosuppressed lines show a gradation of developmental defects and changes in lignin content (40% reduction) and structure (prominent frequency of *p*-hydroxyphenyl units), but content in foliar sinapoyl esters is similar to the control. The purple coloration of their leaves is correlated to the accumulation of sinapoylated anthocyanins.

Plants synthesize a wide variety of natural products based on the phenylpropane skeleton derived from Phe (Petersen et al., 1999). These compounds have an array of important functions, which are not yet fully evaluated or understood and involve a variety of ecological and physiological phenomena (Stafford, 1990; Debeaujon et al., 2000). The derivatives of hydroxycinnamic acids are essential intermediates in lignification and influence the physicochemical properties of the cell walls (Boerjan et al., 2003). Sinapoyl esters function to protect Arabidopsis (*Arabidopsis thaliana*) from UV irradiation (Landry et al., 1995; Booij-James et al., 2000) and caffeoyl and feruloyl esters play a significant role as antioxidants (Grace and Logan, 2000; Mathew and Abraham, 2004). Hydroxycinnamic acids are the precursors of a wide range of volatile compounds with most likely allelochemical functions (Dudareva et al., 2004). Other important groups of natural products derived from phenylpropane units are involved in plant response to environmental biotic and abiotic stimuli. For example, stilbenes and isoflavones are important phytoalexins in plants (Nicholson and Hammerschmidt, 1992).

[1] This work was supported by Genoplante (AF grant no. 2001024), the Human Frontier of Science (programme RG 280/1999M for isolation of the *null cyp98A3* mutant), and the Région Ile de France (SESAME grant). N.A. was supported by the Centre Régional des Oeuvres Universitaires et Scolaires for his Ph.D. thesis.

* Corresponding author; e-mail daniele.werck@ibmp-ulp.u-strasbg.fr; fax 33–3–90–24–19–21.

The author responsible for distribution of materials integral to the findings presented in this article in accordance with the policy described in the Instructions for Authors (www.plantphysiol.org) is: Danièle Werck-Reichhart (daniele.werck@ibmp-ulp.u-strasbg.fr).

[W] The online version of this article contains Web-only data.

[OA] Open Access articles can be viewed online without a subscription.

Article, publication date, and citation information can be found at www.plantphysiol.org/cgi/doi/10.1104/pp.105.069690.

Downloaded from on May 22, 2019 - Published by www.plantphysiol.org
Copyright © 2006 American Society of Plant Biologists. All rights reserved.

Lignin, which originates from the oxidative polymerization of *p*-hydroxycinnamyl alcohols, is a major structural component of secondarily thickened cell walls of tissues with conducting and/or mechanical functions (Lewis and Yamamoto, 1990; Boerjan et al., 2003). Angiosperm lignin is essentially made of guaiacyl (G) and syringyl (S) units, together with weak or trace amount of *p*-hydroxyphenyl (H) units. Three hydroxylations are necessary to form these three units, which are catalyzed by three different cytochrome P450 monooxygenases: cinnamate 4-hydroxylase (C4H or CYP73), *p*-coumaroyl ester 3′-hydroxylase (C3′H or CYP98), and ferulate 5-hydroxylase (F5H or CYP84; Humphreys and Chapple, 2002). The 3-hydroxylation step was only recently shown to involve the cytochrome P450 CYP98A3 in Arabidopsis (Schoch et al., 2001; Franke et al., 2002a, 2002b; Nair et al., 2002). The *meta*-hydroxylation (or 3-hydroxylation) is not catalyzed on the free *p*-coumaric acid as anticipated, but on its conjugates with shikimic or quinic acids (Schoch et al., 2001). CYP98A3, together with the associated hydroxycinnamoyl-CoA:shikimate/quinate hydroxycinnamoyl transferase (HCT; Hoffmann et al., 2003, 2004), controls a major branch point dispatching phenolic precursors between the synthesis of lignin monomers and that of flavonoids, stilbenes, and probably coumarins (Fig. 1).

An ethyl methanesulfonate mutant of the *CYP98A3* gene has recently been described (Franke et al., 2002a, 2002b). The *ref8* mutation was a single missense base change in the last one-third of the coding sequence, which was sufficient to result in a strong impact on plant development and in the inhibition of the formation of sinapoyl esters and of the G and S lignin units. Here we describe isolation of a T-DNA insertion mutant and show that complete inactivation of *CYP98A3* has an even greater impact on plant development. Gene inactivation is associated with reduced cell expansion, altered sugar composition of cell walls, and decreased content in crystalline cellulose and pectins. Changes in plant and cell wall composition are associated with strong perturbations in the expression of genes involved in energetic and stress metabolism, signaling cascades, and cell wall development. In agreement with the results obtained on the *ref8* mutant (Franke et al., 2002a), the lignification of the aerial part of this insertion mutant is deeply altered, with a reduced lignin content essentially made of H units and only trace amounts of G and S units. In contrast to stems, roots of the null mutant, however, display an ectopic lignification phenotype and a substantial frequency of G and S lignin units. Similar to the *ref8* mutant, only trace amounts of sinapoyl malate (SM) are observed in the null mutant, which not only contains unusual *p*-coumaroyl derivatives, but also accumulates flavonol glycosides. To get further insight into the role of *CYP98A3* and plants less severely affected in their development, we also produced cosuppressed plants. Surprisingly enough, while changes in lignification were similar to those observed in the null mutant, albeit less pronounced, our analyses revealed that the leaves of *CYP98A3* cosuppressed plants overaccumulate sinapoylated anthocyanins, and that their levels of SM are similar to the control.

Together, these data indicate (1) an alternative *meta*-hydroxylation pathway leading to G and S units in root lignin and, to a lesser extent, in the rachis; (2) cross talk between hydroxycinnamic acid/lignin and flavonoid pathways; and (3) a crucial role of phenolic precursors for cell wall expansion and homeostasis control during plant development.

RESULTS

cyp98A3 T-DNA Insertion and Cosuppression Mutants Show Drastic Impairments in Growth and Development

A *cyp98A3* insertional mutant was isolated by PCR screening of a T-DNA-mutagenized population in the

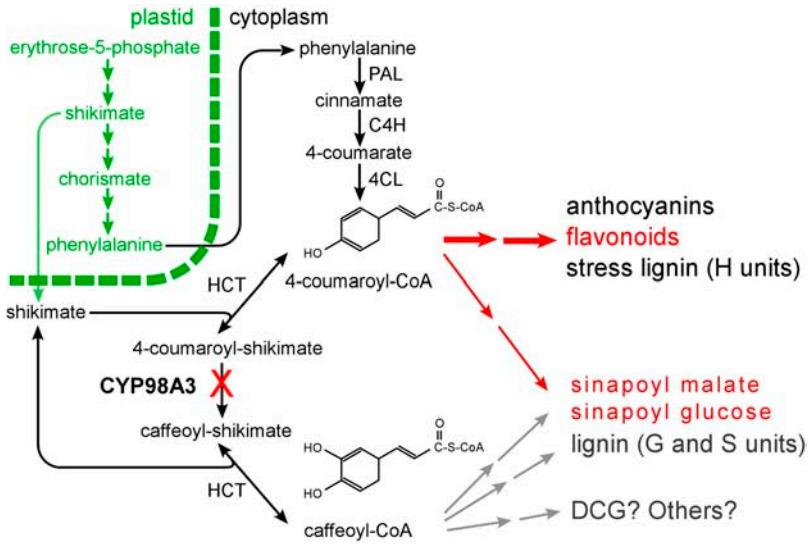

Figure 1. The phenylpropanoid pathway and modification occurring as a result of *CYP98A3* suppression. The pathways activated in the *cyp98A3* mutants are shown in red. The pathways inactivated are shown in gray. The monolignol DCG has been described as a growth regulator (Binns et al., 1987; Tamagnone et al., 1998). Aromatic amino acids, including Phe, are synthesized in the plastids via the so-called shikimate pathway (Herrmann and Weaver, 1999). The mode of transport of shikimate and Phe from the plastids to the cytoplasm is not yet described. 4CL, 4-Hydroxy cinnamoyl-CoA ligase.

Downloaded from on May 22, 2019 - Published by www.plantphysiol.org
Copyright © 2006 American Society of Plant Biologists. All rights reserved.

accession Wassilewskija (Ws) 2 (Krysan et al., 1999) for a T-DNA insertion in the *CYP98A3* locus (At2g40890), as described in ''Materials and Methods.'' A segregation pattern of 3:1 in the progeny of the selfed T1 and T2 mutants, based on kanamycin resistance, and a 1:2:1 segregation (wild-type:heterozygous:homozygous insertion) based on PCR and phenotypic inspection indicated that it contained a single T-DNA insertion locus. Sequencing of the PCR-amplified flanking regions revealed that the T-DNA was inserted in an intron 623 nucleotides downstream of the ATG start codon. Based on PCR amplifications, using a gene-specific primer on either side of the insertion and T-DNA left- and right-border primers, respectively, at least two inverted T-DNAs are present at the insertion site (data not shown). Therefore, a DNA insertion of 12 kb or more in the intron was predicted, which is expected to result in a complete loss of gene function. The total inactivation of the *CYP98A3* gene in homozygous plants was confirmed by RNA-blot hybridization (Fig. 2C) and quantitative reverse-transcription (RT)-PCR (see below). No apparent phenotype was detected for heterozygous *cyp98A3* plants. In contrast, visual examination of the progeny immediately indicated that homozygous plants were severely retarded in their growth (Fig. 2, A and B). In 15-d-old seedlings, the *cyp98A3* mutation resulted in hypocotyls with shortened length (5 ± 1 mm instead of 31 ± 4 mm for the wild type) and increased diameter (1,033 ± 71 μM instead of 711 ± 55 μM for the wild type). Roots had a swollen aspect (576 ± 31 μM diameter instead of 405 ± 23 μM in the wild type) with increased initiation from the crown and showed reduced growth (13 ± 3 mm length instead of 71 ± 7 mm in the wild type) and gravitropism compared to the wild type (Fig. 2A). When transferred to soil, homozygous *cyp98A3* plants maintained their dwarf phenotype with a rosette never exceeding 1 to 1.5 cm in diameter (Fig. 2B). Plants developed a bushy miniature rosette of round leaves and growth of *cyp98A3* plants was arrested latest at the onset of primary stem development, which occurred usually about 2 weeks later than in wild-type plants. Mutants only occasionally initiated bolting stems, which never exceeded 3 cm in height and never developed fertile flowers. Despite this developmental arrest, *cyp98A3* plants can survive for months without growing or showing signs of senescence (data not shown). When grown on soil, homozygous mutants also showed a darker leaf coloration compared to wild-type and heterozygous plants.

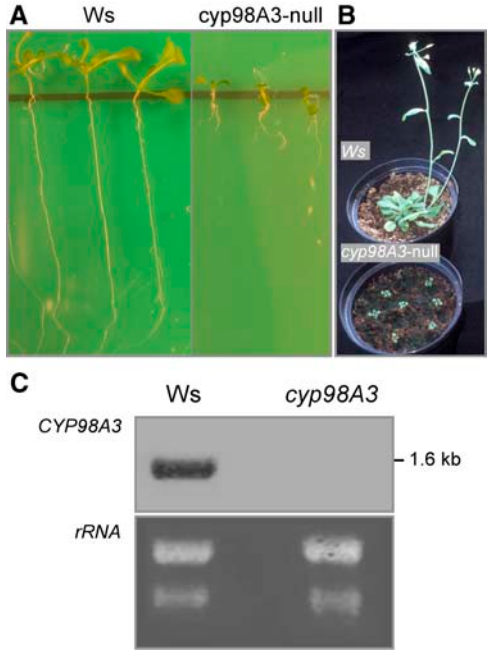

Figure 2. Characterization of *cyp98A3* insertion mutants. A *cyp98A3* insertion mutant was isolated by PCR screening of a T-DNA-mutagenized population in the Ws accession. A, Fifteen-day-old seedlings grown on vertical agar plates. Wild-type Ws plants are shown on the left; homozygous *cyp98A3* mutants on the right. B, Six-week-old null *cyp98A3* insertion plants (bottom) grown on soil compared to wild-type Ws plants (top). C, Fifteen micrograms of total RNA isolated from 15-d-old wild-type Ws and *cyp98A3* insertion plants were used for RNA-blot hybridizations using a *CYP98A3* radiolabeled probe. No *CYP98A3* transcript is detectable in homozygous *cyp98A3* insertion mutants.

The reddish-dark bushy appearance and reduced growth of the homozygous null mutants was also shared by plants where *CYP98A3* overexpression under the control of a 35S promoter led to gene cosuppression. Approximately 10% of primary transformants (ecotype Columbia [Col-0]) containing a cauliflower mosaic virus (CaMV) 35S::*CYP98A3* construct showed a reduced growth phenotype (Fig. 3). These independently transformed plants were arrested at different stages of development. The cosuppression of *CYP98A3* in each primary transformant was confirmed by RNA-blot hybridization (data not shown) and quantitative RT-PCR (see below). A gradation of phenotypes was obtained, which appears to be correlated with the onset of the cosuppression (Fig. 3). Some plants arrested earlier in development did not bolt and showed a very limited growth of the rosette (line IV). For others, bolting was delayed and growth of inflorescence stems was retarded (Fig. 3, B and D, lines V to VIII). When plants bolted, inflorescences showed purple stems and cauline leaves. If flowers developed, they were limp, in most cases male sterile, and only occasionally produced viable seeds (Fig. 3, C–E). A few seeds were recovered from primary transformants designated as lines V, VI, and VII in Figure 3, and *CYP98A3* expression was monitored throughout the life cycle in T2 plants derived from each line (Fig. 3F). Cosuppression was preceded by a phase of *CYP98A3* overexpression for all plants (data not shown), and was fully established only when plants were 5 to 6 weeks old. *CYP98A3* transcript levels were then reduced to undetectable levels within the subsequent 3 weeks (Fig. 3F). In fully cosuppressed plants, no *CYP98A3* transcripts were detectable in RNA-blot analysis, and no protein was detected based on protein-blot analyses using CYP98A3-directed polyclonal

Downloaded from on May 22, 2019 - Published by www.plantphysiol.org
Copyright © 2006 American Society of Plant Biologists. All rights reserved.

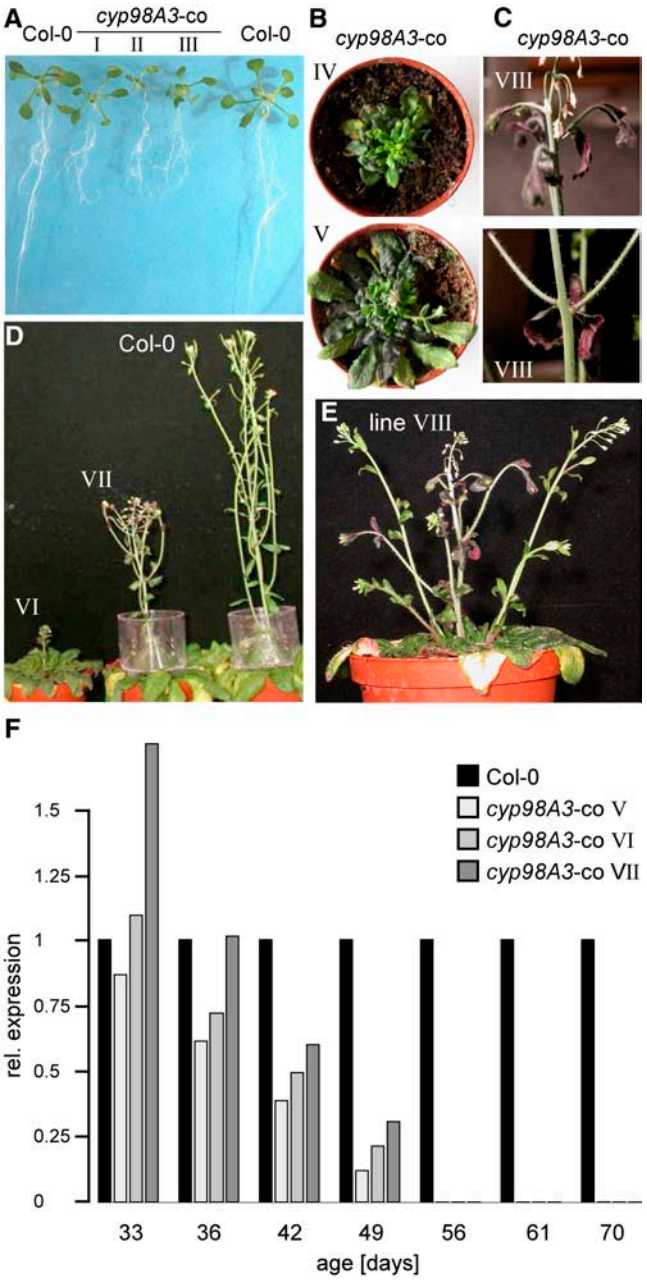

Figure 3. Characterization of cosuppressed *cyp98A3* lines. Arabidopsis Col-0 plants were transformed with a *35S::CYP98A3* construct. Approximately 10% of primary transformants showed cosuppression of *CYP98A3*. The phenotypes of selected transformants are shown in A to E (roman numbers identify individual transformants). A, Three-week-old T1 plants grown on vertical agar plates. Wild-type (Col-0) plants are shown on both sides. B to E, Different 10-week-old cosuppressed T1 lines grown on soil (B). Moderately cosuppressed plants arrested at different stages of bolting stem development (C–E). When plants bolted, inflorescences showed purple stems and cauline leaves; they were limp, in most cases male sterile, and rarely produced viable seeds (C and E). Viable seeds were collected from plants V, VI, and VII (B and D) and progeny derived from these lines was used for quantitative real-time RT-PCR. Plants grown for 4 to 10 weeks were used for total RNA isolation. As an internal standard, *Actin II* was coamplified with the *CYP98A3* cDNA and ΔΔCT values are given relative to the expression level observed for wild-type (Col-0) plants at each time point (F).

antibodies (data not shown). The timing and degree of the cosuppression observed in each cosuppressed line differed slightly and seems to be correlated with the severity of the phenotype, in particular with the onset of developmental arrest.

cyp98A3 Mutants Display Modified Lignin in Stems But Ectopic Lignin Deposition in Roots

Given the severe phenotype of the *cyp98A3* insertion mutant, plants were compared to wild type both at the same age and at a comparable stature. Lignin yield and composition were determined using all aerial parts from insertion mutant plants (6 weeks old) and wild-type Ws plants (6 weeks old or same size as 6-week-old mutants). Lignin determination by the standard Klason gravimetric method could not be applied to the dwarf null plants because this method is too sample demanding. Instead, the lignin structure was analyzed by thioacidolysis, which specifically gives rise to H, G, and S monomers from H, G, or S lignin arylglycerol lignin units involved in β-*O*-4 bonds (Lapierre et al., 1995). The total yield in lignin-derived monomers from dry stems was close to 180 μmol g^{-1} for 6-week-old wild-type and heterozygous *cyp98A3* lines (Table I). These monomers were almost exclusively G and S, with a very low amount of H monomers (close to 1% of the [H+G+S] total). In contrast, thioacidolysis of *cyp98A3* insertion plants resulted in a much lower yield of total monomers (1.5 μmol g^{-1}). In addition, approximately 95% of the thioacidolysis monomers were representative of H units, while G and S monomers were found only in very low, but detectable, amounts (Table I). For comparison purposes, juvenile wild-type plants with a size similar to that of the 6-week-old mutant were subjected to thioacidolysis. Relative to 6-week-old wild-type plants, these juvenile plants yielded 100 times less lignin-derived monomers, which is comparable to the *cyp98A3* insertion mutant. However, the lignin from juvenile wild-type plants was mainly composed of G and S subunits, whereas H units contributed only 3.5% of monomers, compared to 95% in the *cyp98A3* mutant (Table I). Taken together, these results mirror the lignin alteration in the *ref8* mutant caused by a point mutation in *CYP98A3* (Franke et al., 2002a). The drastically low thioacidolysis yield is indicative of very low lignin content. It is also very likely the result of the high frequency of H units in the mutant lignin, since H units have a high tendency to be involved in carbon-carbon or biphenyl-ether interunit bonds that resist thioacidolysis (as also demonstrated by the lignin analyses of the cosuppressed plants). In contrast to the results reported for the *ref8* mutant (Franke et al., 2002a), we could detect weak, but quantifiable, amounts of G and S units in the lignin

Cosuppression was observed starting at 5 weeks for lines V and VI, and increased over time in all lines until no transcripts were detectable at 10 weeks.

Downloaded from on May 22, 2019 - Published by www.plantphysiol.org
Copyright © 2006 American Society of Plant Biologists. All rights reserved.

Table I. *Lignin-derived monomers (H, G, S) after thioacidolysis of dry aerial parts from control Ws and null cyp98A3 mutant*

The data represent the mean value (SE in brackets) of duplicate analyses. Stems/leaves from 6-week-old null plants (grown on soil) or 3-week-old roots (plate grown) were collected and compared to samples either from similarly sized Ws plants or from similarly aged Ws plants.

Sample	Yield in (H + G + S) Monomers	Molar Frequency of Thioacidolysis Monomers		
		H	G	S
	μmol g^{-1} dry sample		*%*	
Dry stems/leaves from				
Six-week-old Ws	162 (8)	0.7 (0.02)	65.7 (0.3)	33.6 (0.2)
Six-week-old heterozygous *cyp98A3*	187 (17)	1.3 (0.1)	67.1 (0.7)	31.6 (0.7)
Ws of same size as below	1.2 (0.4)	3.2 (0.02)	82.1 (1.5)	14.7 (1.6)
Six-week-old homozygous *cyp98A3*	1.5 (0.2)	94.6 (0.2)	2.2 (0.1)	3.2 (0.02)
Dry roots from				
Three-week-old Ws	63 (0.5)	5.2 (0.1)	89.0 (0.2)	5.8 (0.1)
Ws of same size as below	7.5 (0.02)	6.6 (0.7)	85.9 (0.2)	7.5 (0.4)
Three-week-old homozygous *cyp98A3*	1.8 (0.1)	43.1 (9.8)	50.9 (9.9)	6.0 (0.1)

of the *cyp98A3* null mutant (Table I). This important observation constitutes a first indication that the 3-hydroxylation of phenolic compounds might proceed not exclusively via CYP98A3, which is entirely silenced in the null mutant.

Phloroglucinol staining was performed in an attempt to determine the tissue localization of lignin in the insertion mutant. Cytological examination of the miniature inflorescence stems from *cyp98A3* insertion plants was impossible due to the poor mechanical properties of the tissues and crushing of the sections. In contrast, the less severe phenotype of the roots permitted this cytological analysis, and phloroglucinol staining revealed an ectopic lignification phenotype. In addition to xylem cell and fibers, which stain both in wild-type and mutant plant roots, phloroglucinol staining of pith and cortex cells was observed only in the roots of *cyp98A3* insertion mutants (Fig. 4, A and B). A similar ectopic lignification phenotype in roots has been previously reported for various mutants affected in cell wall biogenesis and cell expansion (Caño-Delgado et al., 2000) and in plants treated with inhibitors of cellulose synthase (Caño-Delgado et al., 2003). More surprisingly, an ectopic lignification phenotype was also observed in the rachis (stem, cauline leaves, and sepals) of cosuppressed transformants, which developed bolting stems (Fig. 4, C–E). No phloroglucinol-reactive material was, however, detected in the rosette leaves of cosuppressed plants or in the hypocotyls and rosette leaves of the *cyp98A3* insertion plants. To clarify the nature of the phloroglucinol-reactive material accumulated, we analyzed the lignin content and structure in stems of cosuppressed plants, as well as the structure of root lignin from 3-week-old *cyp98A3* insertion plants. Inflorescence stems of cosuppressed plants were harvested from T2 plants derived from lines V, VI, and VII at an age of 13 weeks, when plant growth was fully arrested and CYP98A3 transcripts were undetectable (Fig. 3F). Due to the limited number of T2 seeds/plants available, material from all three lines was pooled. The extract-free stems of cosuppressed plants were characterized by a 40% reduced Klason lignin content relative to the corresponding Col-0 control (Table II). Upon thioacidolysis, the lignin from cosuppressed plants released H, G, and S monomers in much lower total yield compared to wild type (93% reduction), which is indicative of a high content in resistant

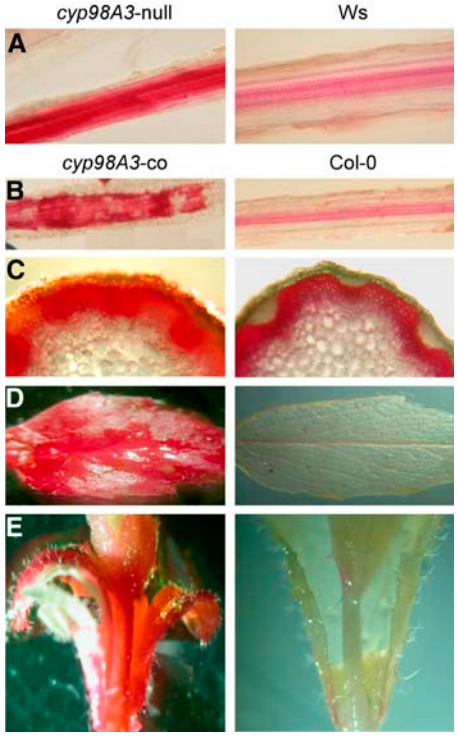

Figure 4. Ectopic lignification phenotypes of *cyp98A3* insertion and cosuppressed plants. Plant material was stained with phloroglucinol and visualized using whole-mount bright-field microscopy. A, Roots from 3-week-old wild-type (Ws) and *cyp98A3* insertion plants (30×). B to E, Different organs from 10-week-old T2 plants derived from the cosuppressed line VII (Fig. 3) were used for phloroglucinol staining. Roots (B, 30×), inflorescence stems (C), cauline leaves (D), and flowers (E, each 10×).

Downloaded from on May 22, 2019 - Published by www.plantphysiol.org
Copyright © 2006 American Society of Plant Biologists. All rights reserved.

Table II. *Lignin content and structure in extract-free and dry stems of control Col-0 and cosuppressed 13-week-old lines*

The data represent the mean value (SE in parentheses) of duplicate analyses. Plant material of cosuppressed plants was derived from pooled T2 lines V, VI, and VII (Fig. 3).

Sample	Klason Lignin Content	Thioacidolysis Yield			
		(H + G + S)	%H	%G	%S
	% by weight	*μmol g^{-1} Klason lignin*			
Col-0	18.48 (0.05)	1,600 (90)	0.7 (0.01)	69 (0.3)	30.3 (0.3)
Cosuppressed	11.65 (0.11)	220 (30)	74 (1)	13 (0.1)	13 (0.1)

interunit bonds. Similar to *cyp98A3* insertion mutants, the cosuppressed plants are characterized by a strong decrease in the relative amounts of S and G units in stems and a dramatic increase in the proportion of H units, which constitute 74% of lignin thioacidolysis monomers compared to less than 1% in stems from wild-type Col-0 plants (Table II). In addition, the dithioketal derivative of *p*-OH coumaraldehyde was obtained in a low, but quantifiable, amount (about 1.3% of the H main monomers), which indicates that *p*-OH-coumaraldehyde end groups occur that could contribute to the positive phloroglucinol staining in stems of cosuppressed plants.

The analyses of wild-type Ws roots confirmed that, compared to the corresponding stem lignin, roots contain relatively less S units and correlatively more G and H units (Sibout et al., 2003), with H units contributing 5% to 7% to the total lignin thioacidolysis monomers, depending on the developmental stage of wild-type plants (Table I). Similar to stems, roots of the *cyp98A3* insertion mutants provided a lower total thioacidolysis yield and a much higher proportion of H monomers (43%) compared to the wild-type roots. However, the frequency of G thioacidolysis monomers released by root lignin was not reduced to the same extent as in the case of lignin derived from stems, and the frequency of S monomers was comparable in wild-type and mutant roots (Table I). Indeed, G and S units in the root tissues of the *cyp98A3* insertion mutant still constitute more than 56% of the thioacidolysis-derived monomers (wild-type roots contain about 94%; Table I). Together with the persistence of G and S lignin units in the mutant stem, this result further supports the occurrence of an alternative 3-hydroxylation mechanism leading to the ectopic root lignin.

Insertion and Cosuppressed *cyp98A3* Lines Accumulate Flavonoids and *p*-Coumaroyl Derivatives, But Sinapoyl Esters Also Persist

To further characterize the impact of the *cyp98A3* mutation on phenolic metabolism, we analyzed soluble phenolics by liquid chromatography (LC)-mass spectrometry (MS) of soluble phenolics. Given the severe phenotype of the insertion mutant, analyses were performed using 15-d-old seedlings when phenotypic differences to wild-type Ws plants are less pronounced. Despite this, the results obtained for *cyp98A3* insertion plants displayed a higher variability than those for control Ws plants grown under the same conditions (Table III). The main *p*-hydroxycinnamic and flavonol derivatives were identified on the basis of their mass and UV spectra (see "Materials and Methods" and supplemental text for details) or, where available, from literature data (Veit and Pauli, 1999; Bloor and Abrahams, 2002; Tohge et al., 2005). In agreement with the qualitative data reported for the leaves of the *ref8* mutant (Franke et al., 2002a), the analysis of insertion plantlets confirmed a drastic decrease in SM and the accumulation of *p*-coumaroyl derivatives. However, it is noteworthy that homozygous insertion mutants are not completely devoid of SM (Fig. 5; Table III). Likewise, *E* and *Z* isomers of sinapoyl Glc (SG),

Table III. *LC-MS determination of soluble phenolics extracted from 15-d-old control (Ws) or null cyp98A3 mutant plants*

The main flavonol glycosides are representatives of kaempferol (K), quercetin (Q), and isorhamnetin (I; see "Materials and Methods"; Fig. 5). The main *p*-hydroxycinnamic derivatives are representatives of SM (*E* and *Z* isomers, identified with authentic compound), SG (*E* and *Z* isomers, putative identification from characteristic SM and UV spectra), and CG (*E* and *Z* isomers, putative identification from characteristic SM and UV spectra). The data represent the mean value (and SE) of triplicate analyses (three series of six plants each). LC-MS quantitative determination was performed on ion chromatograms reconstructed at *m/z* $(M-H)^-$ for each compound and relative to the internal standard (morin) with a response factor (relative concentration to relative surface) arbitrarily set at 1.

Compound	$(M-H)^-$	Ws	Null *cyp98A3*
		ng/mg fresh material	
Flavonol glycosides			
K1	577	102 (7)	259 (96)
K2	593	72 (10)	210 (52)
K3	739	42 (4)	100 (24)
K4	755	40 (2)	153 (43)
Q1	609	70 (15)	205 (38)
Q2	755	11 (2)	35 (5)
Q3	771	31 (4)	98 (6)
I1	623	24 (5)	82 (18)
Total flavonol glycosides		392 (35)	1,142 (275)
Sinapoyl and coumaroyl derivatives			
SM (*E* and *Z*)	339	243 (27)	23 (19)
SG (*E* and *Z*)	385	239 (14)	64 (38)
CG (*E* and *Z*)	325	Tr	225 (53)

Downloaded from on May 22, 2019 - Published by www.plantphysiol.org
Copyright © 2006 American Society of Plant Biologists. All rights reserved.

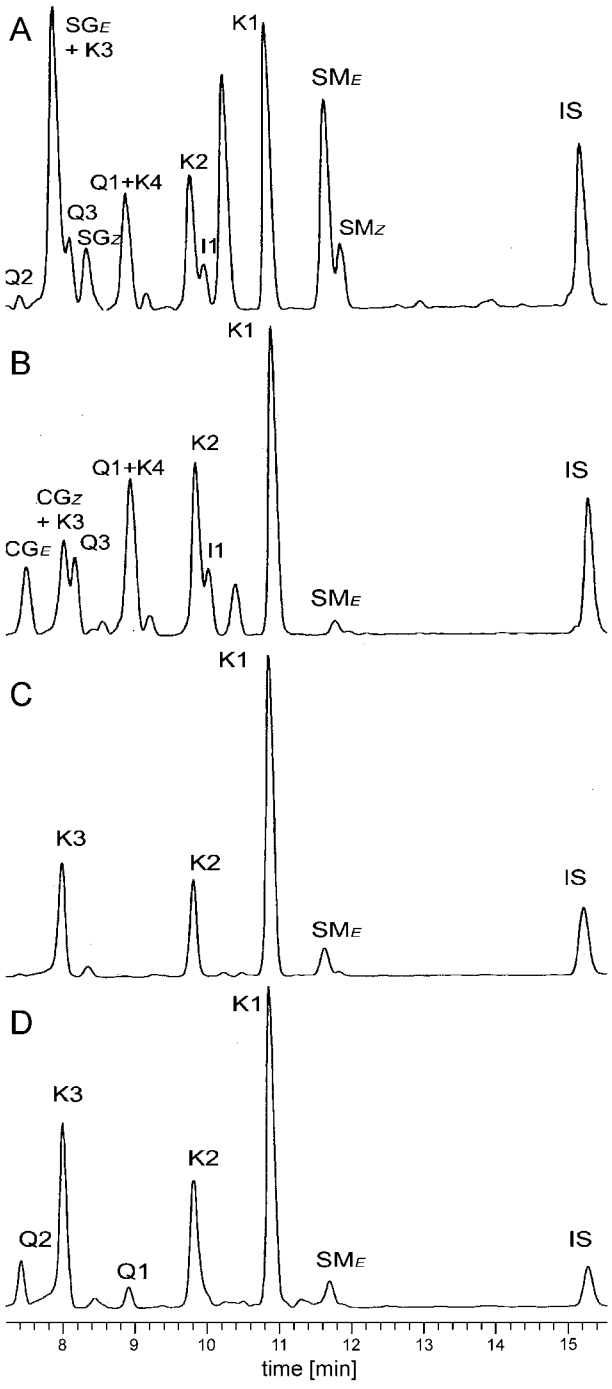

Figure 5. HPLC-MS identification of soluble phenolics extracted from *cyp98A3* insertion and cosuppressed plants compared to wild type. Fifteen-day-old wild-type Ws (A) and *cyp98A3* insertion (B) seedlings were used for MeOH:H_2O (4:1) extraction and liquid chromatography. Cauline leaves from 10-week-old wild-type Col-0 (C) and cosuppressed plants (T2 plants derived from lines V, VI, and VII; Fig. 3; D). For MS, the negative electrospray mode was used and ions were detected in the range from 120 *m/z* to 800 *m/z* (detection: total ion current, arbitrary unit). See "Materials and Methods" and supplemental text for precise peak identification. IS, Internal standard (morin); K, kaempferol; Q, quercetin; I, isorhamnetin.

putatively identified from their mass and UV spectra, were severely reduced, but not abolished, in insertion mutants compared to Ws control plants. Concomitant to this severe decrease of sinapoyl esters, novel compounds were detected in *cyp98A3* insertion plants with mass and UV spectra assignable to *p*-coumaroyl Glc (CG; *E* and *Z* isomers). CG was detected only in trace amounts in wild-type Ws plants (Fig. 5; Table III). In addition, *p*-coumaroyl malate (CM) was observed as a trace component in this series of *cyp98A3* insertion plants, but accumulated to higher amounts in two other sample series (data not shown). No accumulation of *p*-coumaroyl shikimate or *p*-coumaroyl quinate could be detected, as confirmed by the analysis of authentic standards.

The characterization of flavonol glycosides by negative electrospray LC-MS revealed that their level was 3-fold higher in the *cyp98A3* insertion seedlings relative to the Ws control (Fig. 5; Table III). Comparison of the profiles indicates that the mutation leads to a general enrichment of all flavonol glycosides present in wild-type plants and does not seem to induce the increase of selective or specific flavonol derivatives (Table III).

To analyze the role of CYP98A3 in older tissues, pooled cauline leaves from cosuppressed T2 plants derived from lines V, VI, and VII (Fig. 3), which were arrested at later stages of development, were used. Cauline leaves from wild-type Col-0 were analyzed in parallel by negative electrospray LC-MS. In agreement with literature data (Graham, 1988; Pelletier et al., 1999), the flavonol content of mature leaves from wild-type plants was found to be simpler than that of young plants. Only the three major kaempferol glycosides, K1 to K3, were found in significant amounts (Fig. 5C), whereas quercetin derivatives were only trace components. Similar to results with *cyp98A3* insertion plantlets, mature leaves from cosuppressed plants contained 3 times more flavonol glycosides than the corresponding control (data not shown). In addition, quercetin derivatives could be clearly observed on the LC-MS trace of the mutant, while occurring as trace components in the wild type (Fig. 5, C and D). In wild-type plants, these quercetin glycosides are usually observed only at earlier developmental stages (Pelletier et al., 1999) or after UV exposure (Veit and Pauli, 1999). Surprisingly, and in contrast to results obtained with the insertion mutant, the level of SM was not affected in leaves of *cyp98A3* cosuppressed plants (Fig. 5D). Also in contrast to results obtained with *cyp98A3* insertion mutants, CG and CM were observed only in trace amounts in cosuppressed leaves, comparable to levels in wild-type plants.

The deep purple coloration of leaves from cosuppressed plants prompted us also to examine their anthocyanin content by positive electrospray LC-MS. In addition to the major anthocyanin of Arabidopsis, cyanidin 3-*O*-[2′′-*O*-(6′′′-*O*-(sinapoyl) xylosyl) 6′′-*O*-(*p*-*O*-(glucosyl)-*p*-coumaroyl) glucoside] 5-*O*-(6′′′′-*O*-malonyl) glucoside (Bloor and Abrahams, 2002),

Downloaded from on May 22, 2019 - Published by www.plantphysiol.org
Copyright © 2006 American Society of Plant Biologists. All rights reserved.

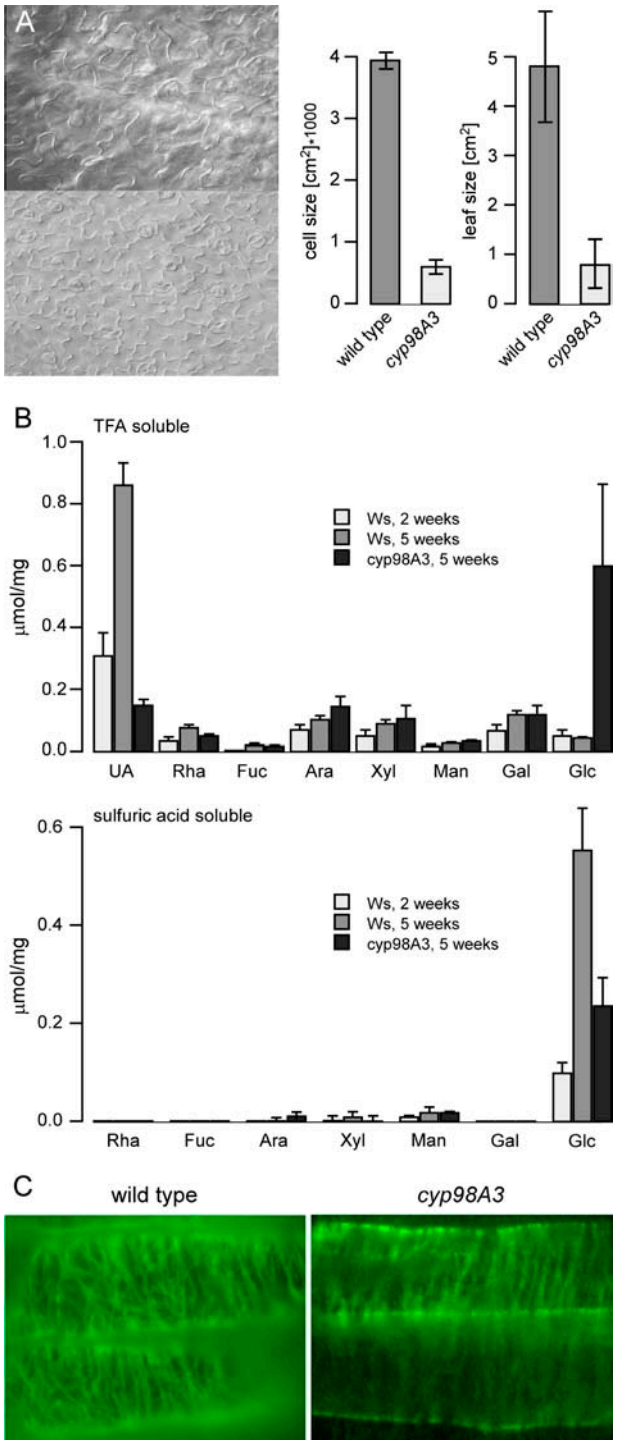

Figure 6. Modifications in cell size and cell wall polysaccharides in *cyp98A3* insertion mutants. A, Reduced epidermal cell size and leaf area in 15-d-old *cyp98A3* insertion mutants compared to wild type (Ws). Fully expanded leaves were stained with Hoyer's solution and were used for Normarski optics microscopy (left). Average cell size was determined using 40 leaf areas from 10 plants. Mean cell sizes and SDS are shown as bar plots (right). Mean of total leaf area size of wild-type and *cyp98A3* insertion plants are shown on the far right. B, Cell wall material was prepared from leaves of 5-week-old *cyp98A3* insertion mutants (white bars), 2-week-old wild-type (Ws; gray bars), and 5-week-old wild-type (black bars) plants. Dried cell wall material was used for TFA hydrolysis (representing matrix polysaccharides) and the resulting monosaccharide derivatives were quantified using gas GC-MS. UA content was determined using the metahydroxyl-biphenyl assay (Blumenkrantz and Asboe-Hansen, 1973). Shown at the top are results from three replicates; error bars indicate SDS. At the bottom, monosaccharide composition of the crystalline cellulose fraction based on Seaman hydrolysis is shown. Dried cell wall material was hydrolyzed using sulfuric acid and the released monosaccharides were quantified using GC-MS. All amounts are shown in micromoles per milligram of dry cell wall material. C, Roots from 2-week-old seedlings were used for immunostaining using tubulin antibodies. Staining of cortical microtubules in the root elongation zone of wild type (Ws) and the *cyp98A3* insertion mutant are shown.

we observed a series of other, less abundant cyanidin derivatives in cosuppressed plants only (data not shown). These are, on the basis of their mass fragmentation pattern, identical to those recently identified by Tohge et al. (2005), who reported the accumulation of such cyanidin derivatives in the leaves of an Arabidopsis mutant overexpressing a MYB transcription factor. All these acylated cyanidin glycosides, which surprisingly include substantial amounts of sinapoylated derivatives, were below the detection level in leaves of wild-type plants.

In summary, the aerial parts of the *cyp98A3* insertion mutant display drastically reduced, although not negligible, levels of sinapoyl esters and S and G lignin units. It is accompanied by a strong increase in *p*-coumaroyl esters, H lignin units, and flavonoids. This confirms the central role of CYP98A3 as the C3′H in the general phenylpropanoid pathway (Schoch et al., 2001; Franke et al., 2002a, 2002b; Nair et al., 2002). However, the persistence of detectable amounts of SM in *cyp98A3* null plants and the presence of G and S lignin units mainly in their roots support the hypothesis of an alternative *meta*-hydroxylase pathway independent of CYP98A3. The occurrence of large amounts of SM and sinapoylated cyanidin glucosides in completely cosuppressed *cyp98A3* plants gives further support to this hypothesis.

Impaired Plant Development of *cyp98A3* Mutants Is Accompanied by Reduced Cell Size and Alteration in Cell Wall Polysaccharide Composition

In an attempt to understand the observed inhibition of plant growth, cell size and cell wall modifications were investigated. A statistical analysis of the size of epidermal cells in different leaves and of different leaf areas indicated a significant 6-fold decrease of the cell size in the *cyp98A3* insertion mutant (Fig. 6A). This reduced cell size is not accompanied by modification of the cell shape, and an estimation of the total number of cells per leaf based on leaf and cell size (Fig. 6A) revealed no difference to wild-type plants. A substantial, but less dramatic, reduction in cell size was also observed in cosuppressed plants (data not shown).

In addition to decreased cell size, an alteration in the cell wall polysaccharide composition was observed

Downloaded from on May 22, 2019 - Published by www.plantphysiol.org
Copyright © 2006 American Society of Plant Biologists. All rights reserved.

(Fig. 6B). Polysaccharide analysis of 5-week-old plants revealed a significant increase in Glc released by trifluoroacetic acid (TFA) hydrolysis representing amorphous glucans (mainly amorphous cellulose). A concomitant decrease in the level of TFA-released uronic acids (UA; reflecting a decrease of pectic polysaccharides) compared to wild-type plants of the same age was observed (Fig. 6B). In addition, the amount of Glc released by Seaman hydrolysis, reflecting crystalline cellulose, was 50% lower in the *cyp98A3* insertion mutant compared to mature Ws plants. It is interesting to note that the decrease in crystalline cellulose is accompanied by an increase in amorphous cellulose in *cyp98A3*, suggesting that the overall amount of cellulose is not altered in cell walls of the mutant, but rather its state of crystallinity, and hence possibly the architecture of the wall. However, at 5 weeks, wild-type plants are significantly larger than *cyp98A3* homozygous plants. To test whether the differences in the composition of the cell wall polysaccharides did not merely reflect delayed development, wild-type plants were grown for 2 weeks until they reached a size comparable to the size of the 5-week-old null *cyp98A3*. Certain changes in polysaccharide composition occur during development of wild-type Ws plants. In mature plants, an increase in UAs was observed, accompanied by a slight increase in all neutral sugars analyzed with the exception of TFA-released Glc. In addition, a strong increase of crystalline cellulose was observed (Fig. 6B), which is likely due to the higher proportion of secondary walls present in the older plants. When comparing *cyp98A3* insertion mutants to both developmental stages of wild-type plants, a reduction of UAs, an increase in amorphous cellulose, and a significant reduction in Ara, reflecting lower levels of arabinogalactan proteins and/or pectin-derived arabinans, was apparent (Fig. 6B).

Cytoskeleton and, in particular, cortical microtubules, are known to be intimately associated with the biogenesis of the cell wall and cellulose microfibril elongation, as well as secondary cell wall depositions and signaling of morphogenetic processes (Baskin, 2001; Wasteneys, 2004). Immunostaining of cortical microtubules in elongating root cells did not reveal any significant perturbation of the transversal orientation of the microtubules. However, the overall microtubule structure was altered and appeared more punctuated (Fig. 6C).

Impaired Development and Reduced Cell Size Is Accompanied by Massive Changes in Gene Expression

The strong alterations in cell wall composition, cell size, and in overall plant development observed in the *cyp98A3* insertion mutant go beyond expectations and cannot be explained by modifications in phenylpropanoid metabolism alone. Gene expression-profiling analyses were thus performed to pinpoint the underlying developmental defects. Given the severe phenotype of the mutant, 15-d-old seedlings grown in vitro were used to minimize the impact of differences in plant development on gene expression and to catch a picture of the phenomenon at its onset. Although even at this early stage pleiotropic and other indirect effects cannot be excluded, they were expected to be less pronounced.

In a preliminary experiment, the expression of selected genes upstream in the phenylpropanoid pathway was compared using quantitative real-time RT-PCR analysis. Given that genes encoding phenylpropanoid enzymes display diurnal changes in their expression (Rogers et al., 2005), we examined expression levels throughout the 12-h light cycle in plants grown under a 12-h-light/12-h-dark regime. In wild-type plants, the transcript levels of all phenylpropanoid genes were highest 4 h into the light period. At the end of the day period, they returned to the same levels observed at 0 h (Fig. 7A). This variation in gene expression is in agreement with studies by Rogers et al. (2005), and a comparable cycling of all transcripts analyzed was also observed in *cyp98A3* insertion mutants, with the exception of a total inactivation of *CYP98A3* (Fig. 7A). While transcript levels of genes encoding Phe ammonia lyase (PAL1; At2g37040) and HCT (At5g48930; Fig. 7A) were comparable in *cyp98A3* mutants and wild type at all time points, an increase in C4H (*CYP73A5*; At2g30490) expression compared to wild type was observed at the 2-, 4-, and 8-h time points in *cyp98A3* insertion mutants (Fig. 7A). In 10-week-old cosuppressed T2 plants derived from the primary transformants V, VI, and VI (Fig. 3), which were arrested in growth when analyzed, *CYP98A3* gene expression is suppressed to undetectable levels (Figs. 7B and 3F). This suppression was accompanied by a decrease in the expression of PAL1, C4H, and HCT at all time points analyzed (Fig. 7B). However, in all cases, cycling during the daylight period was not altered. Cosuppression of the *CYP98A3* gene in adult plants, but not inactivation via a T-DNA insertion in juvenile plantlets, thus appears to result in a repression of the general phenylpropanoid pathway. But the inactivation of *CYP98A3* has no impact on the circadian cycle of phenylpropanoid gene expression. The *cyp98A3* insertion and wild-type Ws lines grown under the same conditions can thus be compared on a larger scale in juvenile plants.

Microarray analysis of gene expression was thus performed using 15-d-old homozygous *cyp98A3* insertion plants compared to wild-type Ws. Two biological replicates were analyzed, with two technical replicates (dye swaps) each for a total of four microarrays. The CATMA Arabidopsis near-full genome array was employed, which contains 24,576 gene-specific elements representing 21,371 annotated genes. Statistical analysis (see ''Materials and Methods'' for details) identified 1,944 elements representing 1,889 annotated genes to be differentially expressed (adjusted p [t test] < 0.05). Among these, 1,067 elements (1,038 genes) changed more than 2-fold, and 362 elements representing 352 annotated genes changed

Downloaded from on May 22, 2019 - Published by www.plantphysiol.org
Copyright © 2006 American Society of Plant Biologists. All rights reserved.

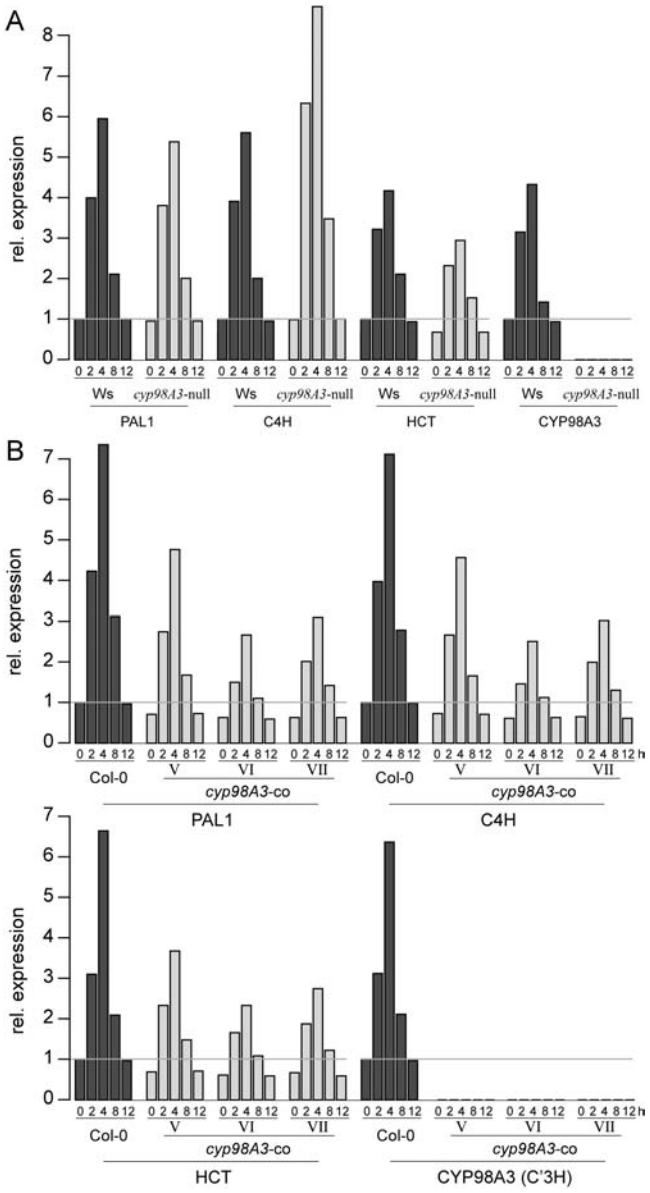

Figure 7. Phenylpropanoid gene expression in *cyp98A3* insertion and cosuppression mutants. A, Fifteen-day-old *cyp98A3* insertion mutant (*cyp98A3* null) and wild-type (Ws) plants were harvested at different time points after the onset of light (time 0 h) during a regular 12-h light period as indicated (plants grown on agar plates under 12-h-light/12-h-dark cycle). Total RNA was used for quantitative real-time RT-PCR. As an internal standard, *Actin II* was coamplified with the *PAL1*, *C4H*, *HCT*, and *CYP98A3* cDNA and ΔΔCT values are given relative to the expression level of the respective gene observed for wild-type (Ws) plants at 0 h. B, Ten-week-old cosuppressed T2 Col-0 plants derived from lines V, VI, and VII (Fig. 3) were used for quantitative real-time RT-PCR. Plants were cultivated on soil under a 12-h-light/12-h-dark cycle. Expression levels of each gene are given relative to the respective level observed for wild-type (Col-0) plants at 0 h.

more than 3-fold (94 genes overexpressed and 260 genes repressed in the mutant).

Supplemental Table I lists normalized expression ratios and annotation details for all differentially expressed genes; the complete dataset was deposited into the ArrayExpress database (accession E-MEXP-346). Functional grouping of differentially expressed genes using the Functional Category Database at MatDB (Schoof et al., 2002; Fig. 8A) indicates a profound modification of plant metabolism. As expected in a mutant almost completely blocked in carbon utilization for lignin synthesis and with a strong phenotype, perturbations in primary metabolism are much more severe than in mutants such as *pal1pal2*, where lignin synthesis is only decreased to 30% (Rohde et al., 2004). Functional groups over-represented in the group of down-regulated genes, which change more than 3-fold, point to a strong repression of light- and oxygen-dependent energy production and carbon fixation, reflected by a decreased expression of plastidal genes involved in photosynthesis and respiration (Fig. 8A). Indeed, several genes encoding proteins involved in the light-harvesting complex (e.g. chlorophyll *a/b*-binding proteins At2g34430, At3g08940, and At3g47470), in photosynthetic electron transport (e.g. the putative ferredoxin At1g10960 and proton gradient regulation 5, At2g05620; Munekage et al., 2002), and in the Calvin cycle (e.g. Rubisco At5g38410 and the putative Rib-5-P isomerase At3g04790) are strongly down-regulated in the mutant compared to the wild type (Supplemental Table I). In contrast, genes expressed to higher levels in *cyp98A3* insertion mutants compared to wild type were over-represented in functional categories covering carbohydrate metabolism and include genes encoding enzymes in glycolysis (e.g. the glyceraldehyde 3-P dehydrogenase, At3g04120), the tricarboxylic acid cycle (e.g. the phospho*enol*pyruvate carboxylase, At3g14940), and other anaerobic metabolisms (alcohol dehydrogenase, At1g77120). Also, functional categories related to defense responses were over-represented (Fig. 8A). Among these were genes known to be transcriptionally induced by insect feeding (the β-glucosidase BGL1, At1g52400; and the lipoxygenase LOX2, At3g45140; Stotz et al., 2000) or wounding/jasmonate (e.g. jasmonate response JR1, At3g16470; Leon et al., 1998). Finally, genes involved in secondary metabolism are over-represented in the group of up-regulated genes (Fig. 8A). It is noteworthy that genes encoding enzymes involved in flavonoid and anthocyanin biosynthesis and transport are expressed to higher levels in the *cyp98A3* insertion mutant; These include chalcone isomerase (CHI, At3g55120), dihydroflavonol 4-reductase (DFR, At5g42800), flavanone 3-hydroxylase (F3H, At3g51240), and gluthation transferase (TT19, At5g17220; Weisshaar and Jenkins, 1998; Kitamura et al., 2004). In contrast, but in agreement with quantitative RT-PCR results (see above), among genes involved in monolignol biosynthesis apart from *CYP98A3*, only *C4H* is differentially expressed, while the expression of all other genes of the phenylpropanoid pathway remains unaltered (ArrayExpress accession E-MEXP-346).

The higher expression of genes related to stress response, in particular mediated by jasmonate, prompted us to dissect the potential involvement of

Downloaded from on May 22, 2019 - Published by www.plantphysiol.org
Copyright © 2006 American Society of Plant Biologists. All rights reserved.

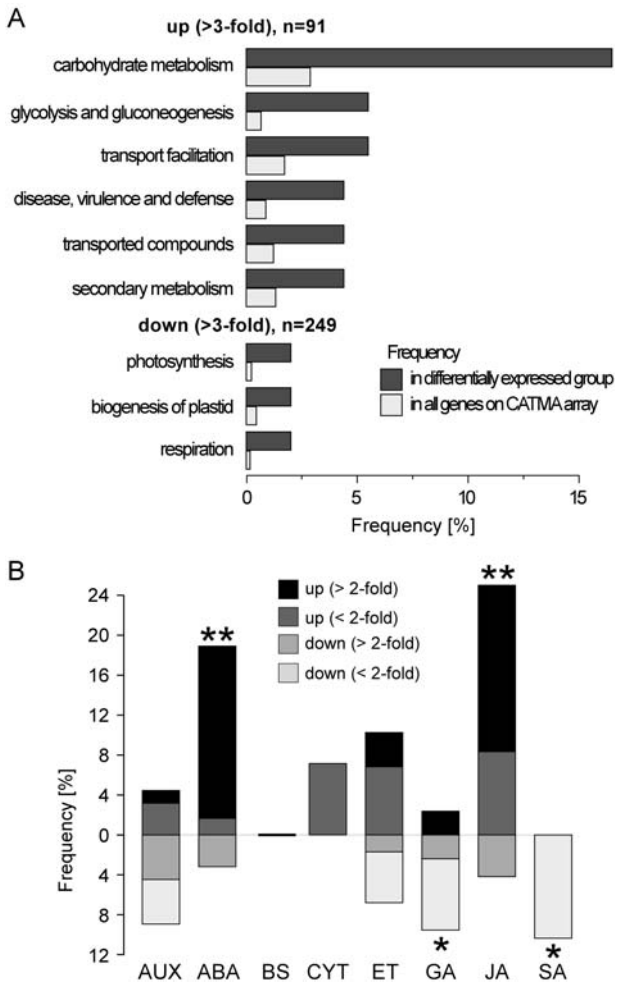

Figure 8. Global changes in gene expression in *cyp98A3* insertion mutants. Wild-type Ws and *cyp98A3* insertion plants grown for 15 d on agar plates were used for total RNA isolation. Microarray analyses were performed using two biological replicates with two technical replicates (dye swaps) each, and the CATMA Arabidopsis near-full genome array. Upon normalization and statistical analysis, 1,889 annotated genes were found to be differentially expressed (Bonferroni-adjusted p [t test] < 0.05). A, Functional grouping of differentially expressed genes that differed in expression more than 3-fold between *cyp98A3* insertion mutants and wild-type Ws using the Functional Category Database at MAtDB (Schoof et al., 2002; http://mips.gsf.de/proj/funcatDB). The frequency of up-regulated genes in each functional category (shown as dark-gray bars) was compared to the frequency of all genes represented on the microarray in the same functional category (shown as light-gray bars). Only functional categories that are over-represented (p [hypergeometric distribution] < 0.05) in the group of up-regulated genes are shown. At the bottom, results of the same analysis for 249 genes, which were expressed to more than 3-fold lower levels in *cyp98A3* mutants and which were annotated in the Functional Category Database, are shown. B, We retrieved from TAIR (Garcia-Hernandez et al., 2002; http://www.arabidopsis.org/tools/bulk/go) curator-annotated lists of genes that were placed into the GO terms ''biosynthesis of,'' ''signal transduction mediated by,'' and ''response to'' the plant hormones auxin (AUX), abscisic acid (ABA), brassinosteroid (BS), cytokinin (CYT), ethylene (ET), gibberellic acid (GA), jasmonic acid (JA), and salicylic acid (SA). Two asterisks indicate over-represented groups (p [hypergeometric distribution] < 0.01), one asterisk indicates $P < 0.05$. Shown as stacked bar plots are the frequencies of genes in each group expressed to higher levels in *cyp98A3* mutants (on top of the vertical axis, separately for genes changing more [black bars] or less [dark-gray bars] than 2-fold), as well as for genes expressed to lower levels in *cyp98A3* insertion plants (below the vertical axis; medium-gray bars indicate less than 2-fold difference, light-gray bars indicate more than 2-fold difference).

this plant hormone and to compare it to the impact of other hormones. Therefore, we retrieved from The Arabidopsis Information Resource (TAIR; Garcia-Hernandez et al., 2002) curator-annotated lists of genes that are involved in the ''biosynthesis of,'' in the ''signal transduction mediated by,'' and in the ''response to'' the plant hormones auxin, abscisic acid, brassinosteroid, cytokinin, ethylene, gibberellic acid, jasmonic acid, and salicylic acid. Within each of these groups of genes, the frequency of differentially expressed genes was determined and compared to the frequency of differentially expressed genes among all genes represented on the array. Genes expressed to higher levels in the *cyp98A3* mutant were clearly over-represented in the functional group related to jasmonate signaling (Fig. 8B). Indeed, many genes involved in the biosynthesis of jasmonate are significantly higher expressed in the mutant compared to wild type (Ws); These include LOX2 (see above), LOX1, allene oxide synthase (CYP74A, At5g42650), and allene oxide cyclase 4 (At1g13280).

In addition, genes related to the abscisic acid cascade are over-represented in the group of genes expressed to higher levels in *cyp98A3* insertion mutants (Fig. 8B). These include the gene responsive to dehydration 22 (*RD22I*, At5g25610), which is strongly induced by abscisic acid and drought (Yamaguchi-Shinozaki and Shinozaki, 1993), and the Arg decarboxylase 2 (*ADC2*, At4g34710) gene, which is strongly activated by abscisic acid, but also by methyl jasmonate and mechanical wounding, and is involved in polyamine biosynthesis (Perez-Amador et al., 2002). Also expressed to higher levels in *cyp98A3* insertion mutants were two homeodomain Leu-zipper transcription factors (ATHB5, At5g65310; and ATHB7, At2g46680) involved in abscisic acid-mediated signaling pathways related to drought and osmotic stress (Söderman et al., 1996) and seed germination (Johannesson et al., 2003), respectively.

None of the other plant hormones analyzed appears to have a similar relevance for the group of genes expressed to higher levels in the *cyp98A3* insertion mutant. To a lesser extent, genes related to gibberellic acid and salicylic acid are more frequently found in the group of genes expressed to lower levels in *cyp98A3* insertion mutants than expected by chance (Fig. 8B). Among genes related to salicylic acid signaling and expressed to lower levels in *cyp98A3* insertion mutants, defective in induced resistance 1 (At5g48485) encodes a lipid transfer protein that, when mutated, results in specific loss of systemic acquired resistance (Maldonado et al., 2002).

Downloaded from on May 22, 2019 - Published by www.plantphysiol.org
Copyright © 2006 American Society of Plant Biologists. All rights reserved.

Finally, in an attempt to explain the dramatic decrease in cell growth and plant development observed in the mutant, we further explored the expression of genes involved in cell expansion and cell division. This analysis revealed that no gene annotated in TAIR gene ontology (GO) term "cell division" is differentially expressed more than 2-fold. In addition, none of the genes involved in the core cell cycle machinery (Vandepoele et al., 2002) is differentially expressed between wild-type and *cyp98A3* mutant plants. In contrast, 12.5% of genes annotated in the GO term "cell growth" are differentially expressed between *cyp98A3* insertion and wild-type plants. Among genes in this group, putative expansins, which mainly act in loosening cell walls for regulating cell expansion (Lee et al., 2001), form the largest group. Six of the 28 expansin family members represented on the array used are differentially expressed, significantly more than expected by chance. However, some expansin isoforms (EXP1, At1g69530; EXP10, At1g26770; and EXPR, At4g17030) are expressed to higher levels in *cyp98A3* insertion mutants, whereas others (EXP8, At2g40610; EXP3, At2g37640; and EXP11, At1g20190) are down-regulated compared to levels found in wild-type plants.

Genetic and Chemical Complementation

To ensure that the observed phenotype, in particular the drastic growth and developmental inhibition of the null mutant, was indeed the result of the *CYP98A3* gene inactivation, a genetic complementation was performed by transformation of heterozygous plants with a construct containing the *CYP98A3* coding region under control of the CaMV 35S promoter. Transformants were identified based on the BASTA resistance marker present in the construct, and homozygous *cyp98A3* plants in the progeny of BASTA-resistant plants were identified using PCR (Fig. 9A). Homozygous *cyp98A3* insertion plants containing the 35S::*CYP98A3* constructs were morphologically indistinguishable from wild-type plants (Fig. 9B). They displayed the same phenotype, including growth and development, as wild-type and heterozygous plants. Based on phloroglucinol staining, no signs of ectopic lignification were detected in roots of complemented plants (data not shown).

The observed growth inhibition in *cyp98A3* insertion plants may result either from a depletion of 3-hydroxylated products or from the accumulation of potentially toxic or bioactive upstream or side products (e.g. flavonoids that were reported to modulate auxin transport [Peer et al., 2004]). In an attempt to dissect these hypotheses, chemical complementation tests were performed. CYP98A3 metabolizes with high efficiency both *p*-coumaroyl shikimate and *p*-coumaroyl quinate, both of which can be generated from *p*-coumaric acid by HCT. HCT is also expected to catalyze the conversion of the CYP98A3 product, caffeoyl shikimate/quinate, to caffeoyl-CoA (Hoffmann et al., 2003; Niggeweg et al., 2004). Complementation was therefore first attempted using the commercially available caffeic acid and caffeoyl quinate (chlorogenic acid). *cyp98A3* insertion plants were grown on media containing these compounds, but no stimulation of plant growth was observed (data not shown). Given that caffeoyl shikimate is likely the major CYP98A3 product in vivo based on catalytic parameters (Schoch et al.,

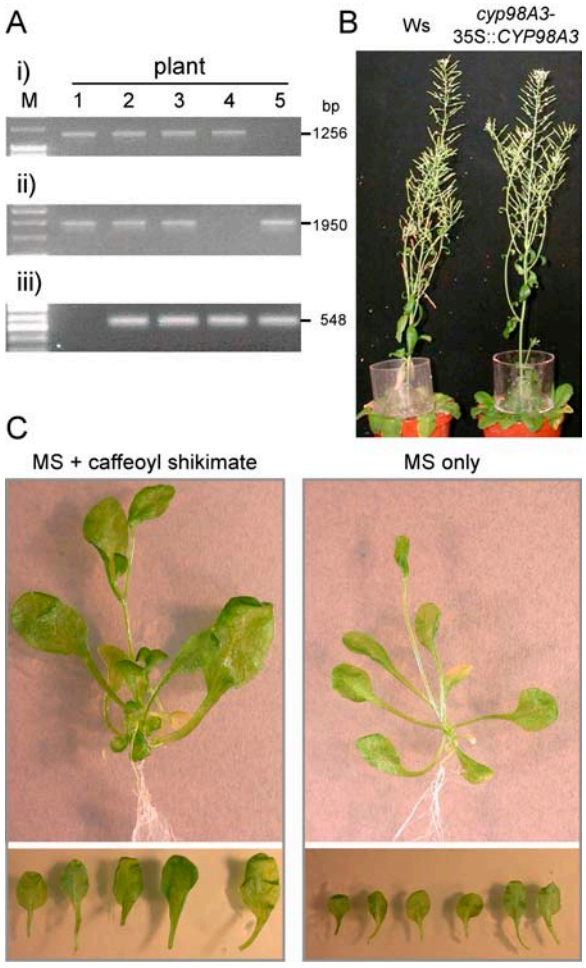

Figure 9. Genetic and chemical complementation of the *cyp98A3* mutation. Heterozygous *cyp98A3* insertion plants were transformed with a CaMV *35S*::*CYP98A3* construct, and homozygous *cyp98A3* plants in the progeny of BASTA-resistant plants were identified using PCR (A) and (i) a gene-specific (Tuc) and a T-DNA-specific (Lbnes) primer; (ii) two gene-specific primers (Tuc, P2) located on each site of the T-DNA insertion site; and (iii) two *35S*::*CYP98A3* construct-specific primers (A3/Bar). Plant 1, Heterozygous, not transformed; plants 2 and 3, heterozygous, transformed; plant 4, homozygous *cyp98A3*, transformed; plant 5, homozygous wild type, transformed. B, Impact of the genetic complementation on 10-week-old plants: wild-type Ws (left) and homozygous c*yp98A3* insertion mutant transformed with the *35S*::*CYP98A3* construct (right). C, Chemical complementation, Homozygous *cyp98A3* insertion mutants grown on Murashige and Skoog medium for 2 weeks were transferred to Murashige and Skoog medium containing 90 μm caffeoyl shikimate and grown for an additional 2 weeks (left). Control plants were transferred to nonsupplemented Murashige and Skoog medium (right).

Downloaded from on May 22, 2019 - Published by www.plantphysiol.org
Copyright © 2006 American Society of Plant Biologists. All rights reserved.

2001; M. Morant, G. Schoch, P. Ullmann, T. Ertunç, D. Little, C.E. Olsen, M. Petersen, J. Negrel, D. Werck-Reichhart, unpublished data), we synthesized this compound enzymatically from *p*-coumaroyl shikimate using recombinant CYP98A3 and purified the product caffeoyl shikimate in sufficient amounts to attempt complementation. Exogenously applied caffeoyl shikimate at least partially restored plant growth (Fig. 9C). Growth inhibition is thus more likely to result from the depletion of an essential 3-hydroxylated product rather than from the accumulation of a toxic precursor. In the absence of a commercially available source of radiolabeled compounds, we cannot exclude a differential uptake of caffeic acid, caffeoyl quinate, and caffeoyl shikimate, but it seems likely that chlorogenic acid or caffeic acid cannot be converted into this essential growth-promoting compound in *cyp98A3* insertion mutants.

DISCUSSION

Analysis of *cyp98A3* Mutants Reveals the Existence of an Alternative *meta*-Hydroxylation Pathway of Phenolic Compounds

The genes belonging to the CYP98 family recently emerged as the cytochrome P450 monooxygenases catalyzing the *meta*-hydroxylation of phenolic compounds in several plant species. These enzymes catalyze the *meta*-hydroxylation of *p*-coumaric derivatives esterified to shikimate, quinate, or phenyllactate (Schoch et al., 2001; Matsuno et al., 2002). In Arabidopsis, CYP98A3 is required for the synthesis of lignin monomers and soluble sinapoyl esters (Franke et al., 2002a). A point mutation in the *CYP98A3* gene was sufficient to completely suppress the production of G and S lignin monomers (as revealed by derivatization followed by reductive cleavage, nitrobenzene oxidation, and analytical pyrolysis) and to drastically reduce the level of soluble *meta*-hydroxylated phenolics in aerial parts of the *ref8* mutant (Franke et al., 2002a, 2002b). It was thus expected that CYP98A3 was the sole 3-hydroxylation enzyme of the phenylpropanoid pathway in Arabidopsis, and that the phenylpropanoid pathway had evolved to exclusively channel the 3-hydroxylation step through *p*-coumaroyl esters and the highly conserved CYP98 enzymes (Schoch et al., 2001; Franke et al., 2002a, 2002b). Our present results challenge this hypothesis.

This analysis of Arabidopsis *cyp98A3* insertion and cosuppressed lines confirms the essential role of CYP98A3 in the synthesis of G and S lignin monomers in aerial parts of the plant and, to some extent, also in the roots. It also confirms that, under normal growth and homeostasis conditions, CYP98A3 is the major contributor to the biosynthesis of soluble sinapoyl derivatives as previously reported by Franke et al. (2002a). However, the *cyp98A3* insertion mutant displays a more dramatic phenotype compared to the *ref8* mutant (Franke et al., 2002b), which suggests that the *ref8* gene still had a low residual activity. In the T-DNA insertion mutant analyzed here, the *CYP98A3* gene is totally inactivated. It nevertheless contains weak, but quantifiable, amounts of G and S units in the lignin of the aerial parts of the plants. G and S units are even more frequent in the ectopic root lignin. Our results, therefore, suggest the occurrence of an alternative *meta*-hydroxylation pathway in Arabidopsis, which seems to be more active in producing the ectopic lignin observed on the roots. It is likely that the same pathway is activated ectopically in the rachis of cosuppressed plants. The detection of SM in the seedlings of the insertion mutant further supports this hypothesis.

It is interesting to note that the alternative *meta*-hydroxylation pathway observed in *cyp98A3* mutants appears to be activated when the prevalent pathway is not functional. However, this alternative pathway cannot complement the defects observed in *cyp98A3* mutants (e.g. reduced growth, reduced lignin in stems, limp stems, and male sterility). It does not ensure normal growth and appears to be active in tissues that do not normally lignify, as judged from the ectopic phloroglucinol staining observed in *cyp98A3* insertion and cosuppressed plants. This alternative pathway seems to be ectopically activated under conditions of perturbed metabolism, but the nature and normal physiological relevance, in specific tissues or at specific stages of plant development, remains to be elucidated. Interestingly enough, the ectopic *CYP98A3* overexpression for complementation of the null mutant does not promote any ectopic lignification. It is worth mentioning that the analysis of precursor conversion by peltate glands isolated from two sweet basil (*Ocimum basilicum*) lines that differ in their ability to produce eugenol also led Gang et al. (2002) to propose the existence of an alternative *meta*-hydroxylation pathway. The line that produced methyl chavicol instead of eugenol had a strongly decreased ability to *meta*-hydroxylate *p*-coumaroyl esters, but an unaltered capability to convert *p*-coumaric acid into caffeic acid. The alternate pathway operating in sweet basil may, however, be different from that producing *meta*-hydroxylated phenolics in the *cyp98A3* mutants from Arabidopsis.

Impact of CYP98A3 Gene Inactivation on Plant Growth and Metabolism

The ectopic activation of an alternative *meta*-hydroxylation pathway in *cyp98A3* mutants is paralleled with strong morphological changes and with an accumulation of flavonoids. The accumulation of flavonoids (flavonol glycosides and anthocyanins) in null and cosuppressed *cyp98A3* mutants is not surprising, since creating a bottleneck at the level of CYP98A3 leads to an accumulation of *p*-coumaroyl-CoA precursors that may subsequently simply overflow into the flavonoid pathway (Fig. 1).

The severe modification in plant development and the complete growth arrest observed in both *cyp98A3*

Downloaded from on May 22, 2019 - Published by www.plantphysiol.org
Copyright © 2006 American Society of Plant Biologists. All rights reserved.

insertion and cosuppressed mutants, however, is more surprising. Given the reduced cell size, which is not accompanied by a reduction of the total number of cells per leaf, these morphological changes are likely due to an inhibition of cellular growth. Consistent with this hypothesis, our microarray analysis revealed no differences in transcript abundance of genes related to the cell cycle, while several genes related to cell expansion are expressed to different levels in wild-type and *cyp98A3* insertion plants. Our data suggest that threshold amounts of *meta*-hydroxylated lignin monomers or of other caffeoyl shikimate-derived compounds are required for normal organization of the cell wall and plant growth. This conclusion is supported by the fact that external application of caffeoyl shikimate complements, at least partially, the growth phenotype of the null mutant. Such a *meta*-hydroxylated derivative might be needed as essential building blocks of the primary cell wall or might more indirectly promote cell wall modifications and growth (e.g. via Ca^{2+} chelation). Alternatively, it may directly act as a growth regulator. Phenolic compounds have been reported to play a role in cell division and expansion, either directly or as components of a cytokinin-dependent signaling cascade (Lynn et al., 1987). A major role in this respect was attributed to dehydrodiconiferyl alcohol glucoside (DCG), which was shown to directly activate cell growth and division in tobacco (*Nicotiana tabacum*) pith, leaves, or cell cultures (Binns et al., 1987; Tamagnone et al., 1998). DCG, as lignin G monomers, is expected to directly derive from CYP98A3 products (Fig. 1). DCG accumulation during plant growth so far has not been described in Arabidopsis. Its ability to restore growth of the null *cyp98A3* mutant will be assessed.

Another possibility is that growth arrest simply results from global perturbations of plant metabolism. A block in lignin biosynthesis suppresses a major carbon sink and induces an accumulation of flavonoids and possibly of indolic derivatives. The latter are stress-related metabolites. Many of the differences in gene expression observed in the *cyp98A3* insertion mutant compared to wild type are reminiscent of a stress response. These include a general downregulation of photosynthesis/chloroplastic genes, indicating reduced energy and carbon assimilation, and elevated expression levels of genes related to defense responses with activation of the jasmonate and abscisic acid signaling pathways. The observed ectopic lignification in roots of the *cyp98A3* insertion mutant and in the rachis of cosuppressed plants can also be considered as indicative of a constitutive induction of a stress response. Ectopic lignification, resulting from mutations in genes encoding cellulose synthase, a chitinase-like enzyme, or a vacuolar ATPase (Schumacher et al., 1999; Caño-Delgado et al., 2000, 2003; Zhong et al., 2002), has been associated with activation of jasmonate and ethylene cascades, with defects in plant growth and cell wall biogenesis, and with stress response. The existence of a link between ectopic lignification and jasmonate cascade was further confirmed by the impact of chemical inhibition of cellulose synthesis with isoxaben, which phenocopies a mutation in cellulose synthase. Isoxaben treatment was reported to induce the jasmonate pathway as well as ectopic lignification (Ellis et al., 2002; Caño-Delgado et al., 2003). Conversely, the combined treatment of wild-type seedlings with jasmonate and 1-aminocyclopopane-carboxylic acid (an ethylene precursor) leads to both reduced cellulose synthesis and ectopic lignification (Caño-Delgado et al., 2003). These changes were correlated with increased expression of the genes involved in stress response and with pathogen resistance (Ellis et al., 2002).

Our data indicate that the defect in the biosynthesis of an essential phenolic component leads to a similar phenotype, including elevated expression levels of genes related to jasmonate signaling, reduced growth, and activation of several stress/defense-related genes. Phenolics thus seem to be one of the elements that relate cell wall biosynthesis with growth promotion and stress signaling. No significant activation of the ethylene signaling pathway was observed in our experiments, but expression profiling indicated higher transcript levels for genes related to abscisic acid signaling in c*yp98A3* mutants. Abscisic acid has been implicated as a signal transduction component in mainly abiotic stress responses, in particular responses to salt, cold, and drought stress (Pastori and Foyer, 2002, and refs. therein), but it has also long been known that abscisic acid inhibits plant growth and is an inducer of dormancy (Koornneef et al., 2002; Xiong and Zhu, 2003). Therefore, it appears plausible that the observed higher levels of transcripts related to abscisic acid signaling may also be related to the observed growth phenotypes, including developmental arrest. In this context, it is noteworthy that *cyp98A3* insertion mutants maintain in a state of developmental arrest and can survive for months without apparent signs of senescence.

What Is the Alternative *meta*-Hydroxylation Pathway?

The proposed alternative *meta*-hydroxylation pathway is not expressed during developmental stem lignification and cannot complement developmental lignification, because mutations in *CYP98A3* lead to an almost complete lack of G and S lignin units in stem (Franke et al., 2002a; Table I). However, it is expressed in tissues of the *cyp98A3* insertion mutant, which normally do not lignify. Together with the increased production of soluble phenolics and stress-related phenylpropanoids, this suggests that the proposed alternative pathway is active under stress conditions and that it is likely a defense-related pathway. Such a hypothesis is supported by the observed activation of genes related to the jasmonate and abscisic acid cascades. The existence of divergent isoforms with separate functions in developmental lignin biosynthesis and in stress-related production of phenolics has

Downloaded from on May 22, 2019 - Published by www.plantphysiol.org
Copyright © 2006 American Society of Plant Biologists. All rights reserved.

been proposed for some enzymes of the phenylpropanoid pathway, e.g. for cinnamoyl-CoA reductase (Lauvergeat et al., 2001). However, it is unlikely that an alternative, stress-related pathway uses the same substrates as CYP98A3, because plants with reduced energy assimilation are not expected to accumulate shikimic or quinic acid in amounts sufficient for allowing their coupling to *p*-coumaric acid. The CoA ester of *p*-coumaric acid or its precursors are, however, expected to accumulate when CYP98A3 and/or shikimate become limiting (Fig. 1), which could also lead to the observed accumulation of flavonoids. Such an accumulation of precursor substrates under stress conditions, or in mutant plants, may allow the activity of an enzyme with low affinity for phenolics to become physiologically relevant. It is also possible that the expression of a specific hydroxylase is activated exclusively under stress conditions. The most obvious candidate genes encoding alternative 3-hydroxylases would be the other members of the CYP98 family. The genes most closely related to *CYP98A3* in Arabidopsis, *CYP98A8* and *CYP98A9*, do not catalyze the *meta*-hydroxylation of any free or conjugated phenolic substrates, including Glc and CoA derivatives (Schoch et al., 2001; M. Morant, G. Schoch, P. Ullmann, T. Ertunç, D. Little, C.E. Olsen, M. Petersen, J. Negrel, D. Werck-Reichhart, unpublished data). However, many other enzymes were previously proposed to catalyze the *meta*-hydroxylation of various phenolic precursors (Schoch et al., 2001, and refs. therein; Franke et al., 2002b, and refs. therein). The production of *meta*-hydroxylated units under stress conditions may rely on one or several of them.

MATERIALS AND METHODS

Isolation of the *cyp98A3* Mutant

An insertion mutant for CYP98A3 was isolated by screening the Alpha collection at the Arabidopsis Knockout Facility at the University of Wisconsin Biotechnology Center (http://www.biotech.wisc.edu/Arabidopsis/Index2.asp; Krysan et al., 1999). Two primers were selected to identify insertions in the *CYP98A3* coding sequences: 98A3F1 (5′-CATGAGCAGCAGCAACAAAAGGTAG-3′) and 98A3R2 (5′-AACATCCAGGTCAGGTACATGTATTTCAC-3′). An insertion was identified in the first intron of *CYP98A3*, and plants heterozygous for the insertion were found in pool 177. The T-DNA contained left borders at both T-DNA junctions based on PCR and DNA sequence analysis.

Construction of the CYP98A3 Overexpression Vector for Genetic Complementation and Cosuppression

The *CYP98A3* cDNA inserted in a pGEM-T vector was amplified using specific primers with added *attB* recombination sites (Gateway Technology; Karimi et al., 2002); sense primer 98A3b1 (5′-GGGGACAAGTTTGTACAAAAAAGCAGGCTATGTCGTGGTTTCTAATAGCGGTG-3′) and antisense primer 98A3b2 (5′-GGGGACCACTTTGTACAAGAAAGCTGGGTTTACATATCGTAAGGCACGCGTTT-3′). The PCR reaction was carried out using as template 200 ng of the plasmid DNA, 10 μM of each primer, and High Fidelity PCR master mix (Roche), according to the recommendations of the manufacturer. After 3 min of heating at 96°C, 18 cycles of amplification were carried out as follows: 1 min denaturation at 95°C, 1 min at 60°C, and 2-min extension at 72°C. The reaction was completed by a 10-min extension at 72°C. The PCR product was purified on a 1% agarose gel and cloned into the pDONR201 donor vector (Invitrogen, Gateway Technology). The ligation mix (20 μL) contained 300 ng of the PCR product, 300 ng of the pDONR201 vector, and BP Clonase reaction buffer, the volume being adjusted to 16 μL with sterile water, according to the instructions of the manufacturer. The reaction was started with 4 μL of BP Clonase enzyme mix. It was incubated at 25°C for 18 h and stopped by 10-min incubation at 37°C with proteinase K (4 μg/20 μL of ligation medium). Electrocompetent bacteria (DH5α) were transformed by electroporation with 1 μL of the ligation medium. Plasmid DNA of positive colonies selected on kanamycin (100 μg/mL) was prepared (NucleoSpin Plasmid) and sequenced for selection of a clone corresponding to the expected sequence. After extraction of the pDONR201 plasmid from the selected clone, the insert was transferred to the destination expression vector pB7WG2 (Karimi et al., 2002) for insertion of the *CYP98A3* cDNA downstream of the CaMV 35S promoter. The reaction was carried out in a 20-μL mix containing 300 ng of pDONR201 with the *CYP98A3* insert, 800 ng of pB7WG2, and LR Clonase buffer, the volume being adjusted to 16 μL with sterile water. Four microliters of LR Clonase enzyme mix were added before incubation at 25°C for 18 h, according to the protocol recommended by the manufacturer. The reaction was stopped by 10-min incubation at 37°C in the presence of proteinase K (4 μg/20 μL of reaction medium). The plasmid DNA (NucleoSpin Plasmid) prepared from the positive colonies selected on spectinomycin (100 μg/mL) was verified by digestion and PCR.

Plant Growth and Transformation

Seeds from Arabidopsis (*Arabidopsis thaliana*) Ws, Col-0, and heterozygous *cyp98A3* mutants were kept at 4°C for 4 d and then washed for 5 min in 70% ethanol. After 20-min incubation with gentle shaking in 20% bleach supplemented with 0.1% Triton X-100, they were washed four times in sterile distilled water and germinated on Murashige and Skoog medium (Duchefa) containing 0.8% Pastagar (Sigma-Aldrich), 1% Suc (Carlo Erba Reagenti), with or without 50 μg/mL kanamycin (Duchefa). Plates were placed in a 21°C growth chamber with a 16-h-light/8-h-dark photoperiod for 15 d.

For plant transformation (genetic complementation and cosuppression), some *cyp98A3* heterozygous mutant or wild-type seedlings were grown on soil at 21°C under a 16-h-light/8-h-dark photoperiod. The pB7WG2 vector was introduced into *Agrobacterium tumefaciens* LBA 4404 virG by electroporation, and stable transformation of the construct in *A. tumefaciens* was confirmed by digestion of the plasmid isolated from the transformants and PCR using T-DNA-specific primers. The plants were then transformed using the floral-dip method (Clough and Bent, 1998).

Seeds from the T0 plants were collected and grown on soil at a density of 1,500 plants per 25 × 50-cm pot. Plants were sprayed with Basta (AgroEvo), 250 mg/L, 5, 14, and 21 d after germination. Transgenic plants resistant to the herbicide were transferred into individual pots and seeds were collected as above. For in vitro selection, seeds of the T1 plants were grown on Murashige and Skoog medium supplemented with 0.8% Pastagar, 1% Suc, 10 μg/mL Basta, and 500 μg/mL carbenicillin.

Circadian rhythm analysis was performed with plants grown under a 12-h-light/12-h-dark cycle in vitro for 15 d for the insertion null mutants and on soil for 10 weeks for the cosuppressed plants.

Analysis of Transgenic Plants by PCR

Segregation analysis and selection of transgenic plants were performed using PCR. Approximately 100 mg of leaf tissue from T1 plants was bulked for DNA isolation using the method described by Fulton et al. (1995). The PCR mixture contained 600 ng of template, 20 pmol of primers, 200 μM dNTPs, 1 × DyNazyme buffer (Finnzyme), 0.5 M betain (*N*,*N*,*N*-trimethyl-glycine; Sigma-Aldrich), and 0.6 units of DNA polymerase (DyNazyme) in a total volume of 25 μL. The following primers were used for testing for the presence of the T-DNA in the *CYP98A3* gene (Fig. 2):

Tuc2 (CYP98A3 promoter region) 5′-AACATCCAGGTCAGGTACATGTATTTCAC-3′; Lbnes (T-DNA left border) 5′-TTGCTTTCGCCTATAAATACGACGGATCG-3′; and P2 (3′ end of the CDS) 5′-GCCAAAGTATGCTCCTCCATGATAGCTCGA-3′. The primers used for testing for the presence of the T-DNA construction in *A. tumefaciens* and in the complemented *cyp98A3* mutants were 98A3 (CYP98A3 CDS) 5′-ACCGGAGGAGATTGACATGTC-3′ and bar (Bar gene) 5′-TCAGTTCCAAACGTAAAACGG-3′.

RNA-Blot Hybridization

Total RNA was extracted from transgenic and wild-type plants using the TRIzol method described by Chomczynski and Sacchi (1987). Total RNA

Downloaded from on May 22, 2019 - Published by www.plantphysiol.org
Copyright © 2006 American Society of Plant Biologists. All rights reserved.

(15 μg/lane) was electrophoresed in 1% agarose-formaldehyde gels and transferred by capillary action onto Zeta-Probe GT genomic tested blotting membranes (Bio-Rad). An 850-bp *CYP98A3* probe was labeled with α-^{32}P-dCTP using the prime-a-gene labeling system (Promega). Prehybridization and hybridization were performed according to instructions provided by the membrane supplier. Equivalent loading of the RNA sample was confirmed by ethidium bromide staining of ribosomal RNA.

Quantitative PCR

Approximately 2.5 μg of total RNA were first reverse transcribed into cDNA. RNA was mixed with 0.5 μg oligo(dT) primers, dNTPs (0.83 mM final), made up to 12 μL with sterile diethyl pyrocarbonate water. The mix was incubated at 65°C for 5 min and kept on ice, before addition of first-strand buffer, 10 mM dithiothreitol, and sterile water to obtain a final volume of 19 μL. One microliter of SuperScript II (200 units/μL) was added, and the reaction incubated 50 min at 42°C, and then 15 min at 70°C for inactivation of the enzyme.

The cDNA resulting from RT was used for real-time quantitative PCR (performed using the TaqMan system on Applied Biosystems GeneAmp 5700 sequence detection system). Couples of primers specific for the genes studied were designed, based on sequences available in GenBank, and according to the following criteria: a size of 20 to 30 nucleotides, a melting temperature around 60°C, and an amplicon size of about 50 to 200 nucleotides. Primers were chosen with the help of Primer Express software (Applied Biosystems; see supplemental text).

For each quantitative PCR, 5 μL of a 5-fold dilution of the cDNA were mixed with the primers, 0.3 μM each, and 13 μL of SYBR Green mix (Applied Biosystems). The volume was adjusted to 25 μL with sterile water and the mix maintained on ice. PCR was initiated with a hot start and a first step at 95°C for 10 min for denaturation, followed by 40 cycles of 15 s at 95°C, and 1 min at 60°C. A first step of sample standardization was performed by quantitative PCR using a constitutively expressed gene for adjustment of cDNA amounts in the PCR reaction. The reference gene used was *Actin II*. The adjusted cDNA dilutions were used for quantification of gene expression. Each quantitative PCR was repeated three times.

Determination of the Area of Epidermal Cells

Leaves were cleared in successive baths of aqueous ethanol (30%, 50%, 70%, 90%, 100%, 100%, and 100%, 30 min each) and left overnight in 100% ethyl ethanol. They were then incubated for 2 h in Hoyer's solution (HCl:Arabic gum:glycerol:water; 100:7.5:5:60). The cells of the epidermal layer were visualized using Nomarski optics (microscope Nikon E800, objective 40× in immersion of oil) and photographed with a digital camera (Sony DXM1200). Average cell areas in different and comparable leaf zones in wild type and mutants were analyzed using ImageJ software (developed at the National Institutes of Health; available at rsb.info.nih.gov.ij).

Preparation of Cell Wall Material and Sugar Composition

Cell wall material was prepared from leaf material (2 or 5 weeks old). Plant tissue was frozen in liquid nitrogen and macerated in 70% ethanol (aqueous) using a Retschmill (Retsch). The ground tissue was pelleted by centrifugation and the resulting pellet washed with chloroform:methanol (1:1, v/v). The pellet was then washed twice with acetone and dried. The cell wall material was hydrolyzed using 2 M TFA and the solubilized monosaccharides were converted into their corresponding alditol acetates followed by gas chromatography (GC)-MS analysis (Albersheim et al., 1967). The UA content was determined using the metahydroxyl-biphenyl assay (Blumenkrantz and Asboe-Hansen, 1973). The crystalline cellulose content was determined using the method described by Updegraff (1969). In brief, cell wall material was incubated with a mixture of acetic acid, nitric acid, and water (8:1:2; v/v) and the supernatant was discarded. The resulting pellet was washed with water until neutral pH and subsequently with acetone until the pellet was dry. The insoluble pellet was dissolved in 72% sulfuric acid (aqueous; Selvendran et al., 1979), shaking for 30 min at room temperature sonication for 15 min and further shaking for 15 min. The sulfuric acid was diluted to 15% with water, incubated for another 2 h, and centrifuged, after which the supernatant was assayed for neutral monosaccharides by GC-MS analysis of their corresponding alditol acetates.

Lignin Histochemistry

Inflorescence stems, leaves, and roots of 10-week-old cosuppressed plants and roots of 3-week-old null seedlings were cleared in ethanol and sectioned with a razor blade (sections cut to approximately 200-μm thickness). The stem sections were stained with phloroglucinol-HCl (Wiesner reagent, 1% [w/v] phloroglucinol in 6 M HCl; Adler et al., 1948) and observed under a microscope.

LC-MS Analyses of Soluble Phenolics

Soluble phenolics from 15-d-old plate-grown seedlings were analyzed as described by Goujon et al. (2003). Briefly, phenolics from whole control (Ws) and homozygous or heterozygous *cyp98A3* and control plants (six plants per assay carefully weighted and three assays per line) were extracted by a prolonged maceration in 2 mL of methanol:water (4:1; v/v) mixture in the presence of morin hydrate (5 μg; Fluka) as internal standard. The extracts were ultrafiltrated (0.45 μm; Millex) before injection (10 μL) into a HPLC-PDA/electrospray ionization-MS system comprising a Finnigan LCQ-DECA mass spectrometer (Thermofinnigan). HPLC was carried out on a HYPURITY C18 column (Thermo-Hypersil; 4.6 mm × 150 mm, particle size 5 μm) at a flow rate of 1 mL/min. The elution was performed using a linear elution gradient from 5% to 60% solvent B (CH_3CN + HCOOH, 0.1%) in solvent A (H_2O + HCOOH, 0.1%) within 30 min. The mass spectral data were collected in the negative mode with the ion trap mass spectrometer equipped with a heated capillary electrospray interface. The sprayer needle voltage was set to 4 kV and the capillary was heated to 350°C. Product peaks were identified by their mass spectrometric fragmentation pattern and relative to data reported in the literature (Veit and Pauli, 1999; Bloor and Abrahams, 2002; Tohge et al., 2005).

The quantitative evaluation of the main identified *p*-hydroxycinnammoyl derivatives and flavonol glycosides was made from ion chromatograms reconstructed at their most specific ion (deprotonated molecule most often) relative to the morin internal standard and with a response factor arbitrarily set at 1 as each flavonol glycoside was not available as an authentic compound. The main flavonol glycosides identified and evaluated herein were kaempferol and quercetin derivatives (Figs. 4 and 5), together with trace amounts of isorhamnetin as detailed in supplemental text. Besides the flavonol glycosides, SM, SG, CG, and CM could be identified from their mass and UV spectra (see supplemental text).

The leaves of Col-0 and of the corresponding 10-week-old cosuppressed plants grown on soil at 21°C under a 16–h-light/8-h-dark photoperiod were also analyzed for their soluble phenolics by electrospray-MS run in the negative mode for the analyses of flavonol and *p*-hydroxycinnamic derivatives and in the positive mode to detect anthocyanins. In addition to the major anthocyanin of Arabidopsis, cyanidin 3-*O*-[2′′-*O*-(6′′′-*O*-(sinapoyl) xylosyl) 6′′-*O*-(*p*-*O*-(glucosyl)-*p*-coumaroyl) glucoside] 5-*O*-(6′′′′-*O*-malonyl) glucoside, identified by Bloor and Abrahams (2002), we could observe a series of other cyanidin derivatives differing from the main one by their acylation mode, as reported by Tohge et al. (2005) in the case of an Arabidopsis mutant overexpressing a MYB transcription factor.

Lignin Analysis

Lignin content and structure of extract-free and dry stems of 10-week-old control Col-0 and of the corresponding cosuppressed plants was determined by the standard Klason method, as described by Dence (1992), and by thioacidolysis, as described by Lapierre et al. (1995), respectively. Lignin structure of dry stems and roots of 6-week-old control Ws and null homozygous *cyp98A3* plants was also investigated using thioacidolysis at an early step of plant development for allowing a better comparison between the wild type and the mutant, which has a very impaired growth and never develops more than aborted inflorescence stems. Thioacidolysis reagent contained 2.5 mL of BF_3 etherate and 10 mL of ethanethiol, adjusted to a 100-mL volume with dioxane. Each dried and ground sample (10–30 mg, analyzed in duplicate experiments) was added to 10 mL of reagent and 1 mL of a docosane solution (0.5 mg/mL in CH_2Cl_2 as GC internal standard) in a glass tube closed with a Teflon-lined screwcap. Thioacidolysis was performed at 100°C for 4 h. The cooled reaction mixture was diluted with 30 mL of water and its pH was adjusted to 3 to 4 with aqueous $NaHCO_3$. The reaction mixture was extracted with CH_2Cl_2 (3 × 30 mL). Combined organic extracts were dried over Na_2SO_4 and then evaporated under reduced pressure at 40°C. The final residue was

Downloaded from on May 22, 2019 - Published by www.plantphysiol.org
Copyright © 2006 American Society of Plant Biologists. All rights reserved.

resolubilized in 1 mL of CH_2Cl_2 before silylation and GC-MS analysis as previously described (Lapierre et al., 1995). The quantitative determination of the main H, G, and S lignin-derived monomers, analyzed as their trimethylsilylated derivatives, was carried out from specific ion chromatograms reconstructed at *m/z* 239 for the H monomers, 269 for G monomers, and 299 for S monomers after an appropriate calibration relative to the docosane internal standard.

Chemical Complementation

Chlorogenic, *p*-coumaric, and caffeic acids were obtained from Sigma-Aldrich. Caffeoyl shikimate was synthesized enzymatically from enzymatically synthesized *p*-coumaroyl shikimate using recombinant CYP98A3 expressed in yeast (*Saccharomyces cerevisiae*; Schoch et al., 2001). The enzymatic conversion was carried out at 27°C for 45 min in several vials, with a final volume of 200 μL for each vial. The assay mixture contained 2 mM *p*-coumaroyl shikimate, 100 pmol of CYP98A3, 0.9 mM NADPH, 0.1 M potassium phosphate, pH 7.4, and a regeneration system (1 mM Glc 6-P and 1 unit Glc 6-P dehydrogenase). The reaction was stopped by acidification with 12 μL of 4 M HCL. The reaction medium was then extracted three times with 1 mL of ethyl acetate. The organic phases were evaporated under argon and the identity of the product was checked by UV spectroscopy and by HPLC analysis as described (Schoch et al., 2001).

To test chemical complementation, 2-week-old *cyp98A3* mutant seedlings were transferred to plates with Murashige and Skoog medium containing 90 μM of the tested compounds for 2 more weeks.

Transcriptome Studies

The microarray analysis has been performed using the CATMA array containing 24,576 gene-specific tags from Arabidopsis (Crowe et al., 2003; Hilson et al., 2004). The gene-specific tag amplicons were purified on Multiscreen plates (Millipore) and resuspended in Tris-EDTA-dimethyl sulfoxide at 100 ng/μL. The purified probes were transferred to 1,536-well plates with a Genesis workstation (Tecan) and spotted on UltraGAPS slides (Corning) using a Microgrid II (Genomic Solution). The current CATMA version printed at the Unité de Recherche Génomique Végétale consists of three metablocks, each composed of 64 blocks of 144 spots. A block is a set of spots printed with the same print tip, which is used three times to create three metablocks. For transcriptome studies, total RNA from around 1 g of whole-plant material from 15-d-old wild-type Ws and cyp98A3 null plants (grown on Murashige and Skoog plates at 21°C with a 16-h-light/8-h-dark photoperiod) were extracted using the TRIzol (Invitrogen) method as described by Chomczynski and Sacchi (1987) followed by two ethanol precipitations, then checked for RNA integrity with the Bioanalyzer from Agilent. Two biological replicates with independent dye swaps were performed for each comparison. cRNAs were produced from 2 μg of total RNA from each pool with the Message Amp aRNA kit (Ambion). Then 5 μg of cRNAs were reverse transcribed in the presence of 200 units of SuperScript II (Invitrogen), Cy3-dUTP, and Cy5-dUTP (NEN) according to Puskas et al. (2002) for each slide. Samples were combined, purified, and concentrated with YM30 Microcon columns (Millipore). Slides were prehybridized for 1 h and hybridized overnight at 42°C in 25% formamide, 5× CCS, 1% SDS. Slides were washed at room temperature in 2× SSC + 0.1% SDS for 4 min, 1× SSC for 4 min, 0.2× SSC for 4 min, 0.05× SSC for 1 min, and dried by centrifugation. Four hybridizations (two dye swaps) were carried out. The arrays were scanned on a GenePix 4000A scanner (Axon Instruments) and images were analyzed using the GenePix Pro 3.0 software (Axon Instruments).

Statistical Analysis of Microarray Data

Statistical analysis was performed as described in Lurin et al. (2004) based on two dye swaps, i.e. four arrays each containing the 24,576 gene-specific tags and 384 controls. The controls were used for assessing the quality of the hybridizations, but were not included in the statistical tests. For each array, the raw data comprised the logarithm of median feature pixel intensity at a wavelength of 635 nm (red) and 532 nm (green). No background was subtracted. First, we excluded spots that were considered badly formed features by manual inspection. Then we performed a global intensity-dependent normalization using the LOESS procedure (Yang et al., 2002) to correct the dye bias, thus generating four sets of $\log_2$ ratios comparing mutant and control. Finally, on each block, the log-ratio median is subtracted from each value of the log ratio of the block to correct for print-tip effects in each metablock. To determine differentially expressed genes, we performed a paired *t* test on the log ratios. The number of observations per spot varies between 2 and 4 and is therefore inadequate for calculating a gene-specific variance. For this reason, we assume that the variance of the log ratios is the same for all genes and adjusted the parametric *P*-values by the Bonferroni method, which controls the family wise error rate. Differentially expressed genes (adjusted p [*t* test] < 0.05) between mutant and wild type were divided into groups of up- and down-regulated genes (mutant/wild type). Upon removal of duplicates and elements lacking a locus annotation (Atxgxxxxx), these genes were used to search the Functional Category Database at MAtDB (mips.gsf.de/proj/funcatDB; Schoof et al., 2002). The frequency of differentially expressed genes that change more than 3-fold in each functional category was compared to the frequency of all genes represented on the microarray using a hypergeometric distribution and only categories that contain more than three gene entries and are over-represented in the group of differentially expressed genes (p [hyper] < 0.01) were retained. Using the same statistical analysis, the frequency of differentially expressed genes that have been placed in selected groups of GO categories was compared to the frequency of all genes on the array in these GO terms. Curator-annotated genes placed in the GO terms ''involved in the metabolism of,'' ''involved in the signaling mediated by,'' or ''involved in the response to'' the hormones auxin, abscisic acid, brassinosteroid, cytokinin, ethylene, gibberellic acid, jasmonic acid, and salicylic acid, respectively, were retrieved from TAIR database (Arabidopsis.org; Garcia-Hernandez et al., 2002). Gene lists related to each hormone were combined and duplicate entries in each group were removed prior to statistical analysis.

Immunofluorescence Visualization of the Microtubules

Whole 15-d-old seedlings were fixed in 1.5% (v/v) formaldehyde and 0.5% (v/v) glutaraldehyde in PEMT buffer (50 mM PIPES, 2 mM EGTA, 2 mM $MgSO_4$, 0.05% [v/v] Triton X-100, pH 7.2) for 40 min, and rinsed in PEMT buffer three times for 10 min. The samples were subsequently digested with 0.05% (w/v) Pectolyase Y-23 (Kikkoman) in PEM buffer (50 mM PIPES, 2 mM EGTA, 2 mM $MgSO_4$) with 0.4 M mannitol for 20 min, rinsed in PEM buffer three times, treated with 220°C methanol for 10 min, and rehydrated in phosphate-buffered saline (PBS; 136 mM NaCl, 6 mM Na_2HPO_4, 2.7 mM KCl, 1.5 mM KH_2 PO_4, pH 7.0) for 10 min. Autofluorescence caused by free aldehydes from glutaraldehyde fixation was reduced with 1 mg/mL $NaBH_4$ in PBS for 20 min, followed by a treatment with 50 mM Gly in PBS (incubation buffer) for 30 min. Seedlings were incubated with primary antibodies against tubulin at 4°C overnight, rinsed in incubation buffer three times for 10 min, and secondary antibodies were applied for 3 h at 37°C. After rinsing in PBS three times, roots were cut off from the rest of seedlings and mounted in 0.1% (w/v) paraphenylene diamine in 1:1 PBS:glycerol, pH 9. Cut cover glasses were used to space slide and cover glasses so as to avoid crushing delicate root tips.

Antitubulin (product N357; Amersham) was used at a dilution of 1:1,000 for this study. Fluorescein isothiocyanate-conjugated anti-mouse IgG (Silenus/Amrad Biotech), diluted 1:100, was used as a secondary antibody.

Immunofluorescence images were collected with an MRC-Bio-Rad 600 (Microscience Division) confocal laser-scanning microscope, coupled to a Zeiss Axiovert IM-10 inverted microscope. Excitation at 488 nm with an argon ion laser was used for fluorescein isothiocyanate fluorochromes. Images were collected using a Plan Neofluar 100× objective lens, N.A. 1.30, following Kalman averaging of six full scans. Images were processed with image-processing software programs including COMOS 7.0 (Microscience Division), confocal assistant 4.02 (written by Todd Clark Brelje), and Adobe Photoshop 4.0 (Adobe Systems).

Sequence data from this article can be found in the GenBank/EMBL data libraries under accession number NM_180006.

ACKNOWLEDGMENTS

We thank Frans Tax and Ken Feldmann (University of Arizona, Tucson, AZ) for isolation of the *cyp98A3* T-DNA insertion mutant and critical reading of the manuscript. The technical support of Marta Ramel is gratefully acknowledged. We sincerely thank Laurent Cezard for performing the thioacidolysis experiments and the INRA for the LC-MS equipment.

Downloaded from on May 22, 2019 - Published by www.plantphysiol.org
Copyright © 2006 American Society of Plant Biologists. All rights reserved.

Received August 19, 2005; revised November 4, 2005; accepted November 5, 2005; published December 23, 2005.

LITERATURE CITED

Adler E, Bjorkquist KJ, Haggroth S (1948) Ûber die Ursache der Farbreaktionen des Holzes. Acta Chem Scand **2:** 93–94

Albersheim P, Nevins DJ, English PD, Karr A (1967) A method for the analysis of sugars in plant cell-wall polysaccharides by gas-liquid chromatography. Carbohydr Res **5:** 340–345

Baskin TI (2001) On the alignment of cellulose microfibrils by cortical microtubules: a review and a model. Protoplasma **215:** 150–171

Binns AN, Chen RH, Wood HN, Lynn DG (1987) Cell division promoting activity of naturally occurring dehydrodiconiferyl glucosides: Do cell wall components control cell division? Proc Natl Acad Sci USA **84:** 980–984

Bloor SJ, Abrahams S (2002) The structure of the major anthocyanin in *Arabidopsis thaliana*. Phytochemistry **59:** 343–346

Blumenkrantz N, Asboe-Hansen G (1973) New methods for quantitative determination or uronic acids. Anal Biochem **54:** 484–489

Boerjan W, Ralph J, Baucher M (2003) Lignin biosynthesis. Annu Rev Plant Biol **54:** 519–546

Booij-James IS, Dube SK, Jansen MAK, Edelman M, Mattoo AK (2000) Ultraviolet-B radiation impact light-mediated turnover of the photosystem II reaction center heterodimer in Arabidopsis mutants altered in phenolic metabolism. Plant Physiol **124:** 1275–1283

Caño-Delgado A, Penfield S, Smith C, Catley M, Bevan M (2003) Reduced cellulose synthesis invokes lignification and defense responses in *Arabidopsis thaliana*. Plant J **34:** 351–362

Caño-Delgado AI, Metzlaff K, Bevan MW (2000) The *eli1* mutation reveals a link between cell expansion and secondary cell wall formation in *Arabidopsis thaliana*. Development **127:** 3395–3405

Chomczynski P, Sacchi N (1987) Single step method of RNA isolation by guanidinum thiocyanate-phenol-chloroform extraction. Anal Biochem **162:** 156–159

Clough SJ, Bent AF (1998) Floral dip: a simplified method for *Agrobacterium*-mediated transformation of *Arabidopsis thaliana*. Plant J **16:** 735–743

Crowe ML, Serizet C, Thareau V, Aubourg S, Rouze P, Hilson P, Beynon J, Weisbeek P, van Hummelen P, Reymond P, et al (2003) CATMA: a complete Arabidopsis GST database. Nucleic Acids Res **31:** 156–158

Debeaujon I, Leon-Kloosterziel KM, Koornneef M (2000) Influence of the testa on seed dormancy, germination, and longevity in Arabidopsis. Plant Physiol **122:** 403–413

Dence CW (1992) The determination of lignin. *In* SY Lin, CW Dence, eds, Methods in Lignin Chemistry. Springer-Verlag, New York, pp 33–61

Dudareva N, Pichersky E, Gershenzon J (2004) Biochemistry of plant volatiles. Plant Physiol **135:** 1893–1902

Ellis C, Karafyllidis I, Wasternack C, Turner JG (2002) The Arabidopsis mutant cev1 links cell wall signaling to jasmonate and ethylene responses. Plant Cell **14:** 1557–1566

Franke R, Hemm MR, Denault JW, Ruegger MO, Humphreys JM, Chapple C (2002a) Changes in secondary metabolism and deposition of an unusual lignin in the *ref8* mutant of *Arabidopsis*. Plant J **30:** 47–59

Franke R, Humphreys JM, Hemm MR, Denault JW, Ruegger MO, Cusumano JC, Chapple C (2002b) The *Arabidopsis REF8* gene encodes the 3-hydroxylase of phenylpropanoid metabolism. Plant J **30:** 33–45

Fulton TM, Chunwongse J, Tanksley SD (1995) Microprep protocol for extraction of DNA from tomato and other herbaceous plants. Plant Mol Biol **13:** 207–209

Gang DR, Beuerle T, Ullmann P, Werck-Reichhart D, Pichersky E (2002) Differential production of *meta*-hydroxylated phenylpropanoids in sweet basil peltate glandular trichomes and leaves is controlled by the activities of specific acyltransferases and hydroxylases. Plant Physiol **130:** 1536–1544

Garcia-Hernandez M, Berardini TZ, Chen G, Crist D, Doyle A, Huala E, Knee E, Lambrecht M, Miller N, Mueller LA, et al (2002) TAIR: a resource for integrated Arabidopsis data. Funct Integr Genomics **2:** 239–253

Goujon T, Minic Z, Amrani AE, Lerouxel O, Aletti E, Lapierre C, Joseleau JP, Jouanin L (2003) AtBXL1, a novel higher plant (*Arabidopsis thaliana*) putative beta-xylosidase gene, is involved in secondary cell wall metabolism and plant development. Plant J **33:** 677–690

Grace SC, Logan BA (2000) Energy dissipation and radical scavenging by the plant phenylpropanoid pathway. Philos Trans R Soc Lond B Biol Sci **355:** 1499–1510

Graham TL (1988) Flavonoids and flavonol glycoside metabolism in *Arabidopsis*. Plant Physiol Biochem **36:** 135–144

Herrmann KM, Weaver LM (1999) The shikimate pathway. Annu Rev Plant Physiol Plant Mol Biol **50:** 473–503

Hilson P, Allemeersch J, Altmann T, Aubourg S, Avon A, Beynon J, Bhalerao RP, Bitton F, Caboche M, Cannoot B, et al (2004) Versatile gene-specific sequence tags for Arabidopsis functional genomics: transcript profiling and reverse genetics applications. Genome Res **14:** 2176–2189

Hoffmann L, Besseau S, Geoffroy P, Ritzenthaler C, Meyer D, Lapierre C, Pollet B, Legrand M (2004) Silencing of hydroxycinnamoyl-coenzyme A shikimate/quinate hydroxycinnamoyltransferase affects phenylpropanoid biosynthesis. Plant Cell **16:** 1446–1465

Hoffmann L, Maury S, Martz F, Geoffroy P, Legrand M (2003) Purification, cloning and properties of an acyltransferase controlling shikimate and quinate ester intermediates in phenylpropanoid metabolism. J Biol Chem **278:** 95–103

Humphreys JM, Chapple C (2002) Rewriting the lignin roadmap. Curr Opin Plant Biol **5:** 224–229

Johannesson H, Wang Y, Hanson J, Engström P (2003) The *Arabidopsis thaliana* homeobox gene ATHB5 is a potential regulator of abscisic acid responsiveness in developing seedlings. Plant Mol Biol **51:** 719–729

Karimi M, Inze D, Depicker A (2002) GATEWAY vectors for Agrobacterium-mediated plant transformation. Plant Sci **7:** 193–195

Kitamura S, Shikazono N, Tanaka A (2004) TRANSPARENT TESTA 19 is involved in the accumulation of both anthocyanins and proanthocyanidins in Arabidopsis. Plant J **37:** 104–114

Koornneef M, Bentsink L, Hilhorst H (2002) Seed dormancy and germination. Curr Opin Plant Biol **5:** 33–36

Krysan PJ, Young JC, Sussman MR (1999) T-DNA as an insertional mutagen in Arabidopsis. Plant Cell **11:** 2283–2290

Landry LG, Chapple CCS, Last R (1995) Arabidopsis mutants lacking phenolic sunscreens exhibit enhanced ultraviolet-B injury and oxidative damage. Plant Physiol **109:** 1159–1166

Lapierre C, Pollet B, Rolando C (1995) New insight into the molecular architecture of hardwood lignins chemical degradative methods. Res Chem Intermediates **21:** 397–412

Lauvergeat V, Lacomme C, Lacombe E, Lasserre E, Roby D, Grima-Pettenati J (2001) Two cinnamoyl-CoA reductase (CCR) genes from *Arabidopsis thaliana* are differentially expressed during development and in response to infection with pathogenic bacteria. Phytochemistry **57:** 1187–1195

Lee Y, Choi D, Kende H (2001) Expansins: ever-expanding numbers and functions. Curr Opin Plant Biol **4:** 527–532

Leon J, Rojo E, Titarenko E, Sanchez-Serrano JJ (1998) Jasmonic acid-dependent and -independent wound signal transduction pathways are differentially regulated by Ca^{2+}/calmodulin in Arabidopsis thaliana. Mol Gen Genet **258:** 412–419

Lewis NG, Yamamoto E (1990) Lignin: occurrence, biogenesis and biodegradation. Annu Rev Plant Physiol Plant Mol Biol **41:** 455–496

Lurin C, Andres C, Aubourg S, Bellaoui M, Bitton F, Bruyere C, Caboche M, Debast C, Gualberto J, Hoffmann B, et al (2004) Genome-wide analysis of Arabidopsis pentatricopeptide repeat proteins reveals their essential role in organelle biogenesis. Plant Cell **16:** 2089–2103

Lynn DG, Chen RH, Manning KS, Wood HN (1987) The structural characterization of endogenous factors from *Vinca rosea* crown gall tumors that promote cell division of tobacco cells. Proc Natl Acad Sci USA **84:** 615–619

Maldonado AM, Doerner P, Dixon RA, Lamb CJ, Cameron RK (2002) A putative lipid transfer protein involved in systemic resistance signalling in Arabidopsis. Nature **419:** 399–403

Mathew S, Abraham TE (2004) Ferulic acid: an antioxidant found naturally in plant cell walls and feruloyl esterases involved in its release and their applications. Crit Rev Biotechnol **24:** 59–83

Matsuno M, Nagatsu A, Ogihara Y, Ellis BE, Mizukami H (2002) *CYP98A6* from *Lithospermum erythrorhizon* encodes 4-coumaroyl-4′-hydroxyphenyllactic acid 3-hydroxylase involved in rosmarinic acid biosynthesis. FEBS Lett **514:** 219–224

Downloaded from on May 22, 2019 - Published by www.plantphysiol.org
Copyright © 2006 American Society of Plant Biologists. All rights reserved.

Munekage Y, Hojo M, Meurer J, Endo T, Tasaka M, Shikanai T (2002) PGR5 is involved in cyclic electron flow around photosystem I and is essential for photoprotection in Arabidopsis. Cell **110:** 361–371

Nair RB, Xia Q, Kartha CJ, Kurylo E, Hirji RN, Datla R, Selvaraj G (2002) Arabidopsis CYP98A3 mediating aromatic 3-hydroxylation: developmental regulation of the gene, and expression in yeast. Plant Physiol **130:** 210–220

Nicholson RL, Hammerschmidt R (1992) Phenolic compounds and their role in disease resistance. Annu Rev Phytopathol **30:** 369–389

Niggeweg R, Michael AJ, Martin C (2004) Engineering plants with increased levels of the antioxidant chlorogenic acid. Nat Biotechnol **22:** 746–754

Pastori GM, Foyer CH (2002) Common components, networks, and pathways of cross-tolerance to stress: the central role of ''redox'' and abscisic acid-mediated controls. Plant Physiol **129:** 460–468

Peer WA, Bandyopadhyay A, Blakeslee JJ, Makam SN, Chen RJ, Masson PH, Murphy AS (2004) Variation in expression and protein localization of the PIN family of auxin efflux facilitator proteins in flavonoid mutants with altered auxin transport in *Arabidopsis thaliana*. Plant Cell **16:** 1898–1911

Pelletier MK, Burbulis IA, Winkel-Shirley B (1999) Disruption of specific flavonoid genes enhances the accumulation of flavonoid enzymes and end-products in *Arabidopsis* seedlings. Plant Mol Biol **40:** 45–54

Perez-Amador MA, Leon J, Green PJ, Carbonell J (2002) Induction of the arginine decarboxylase ADC2 gene provides evidence for the involvement of polyamines in the wound response in Arabidopsis. Plant Physiol **130:** 1454–1463

Petersen M, Strack D, Matern U (1999) Biosynthesis of phenylpropanoïds and related compounds. *In* M Wink, ed, Biochemistry of Plant Secondary Metabolism, Annual Plant Reviews. CRC Press, Boca Raton, FL, pp 151–221

Puskas LG, Zvara A, Hackler L Jr, Van Hummelen P (2002) RNA amplification results in reproducible microarray data with slight ratio bias. Biotechniques **32:** 1330–1334

Rogers LA, Dubos C, Cullis IF, Surman C, Poole M, Willment J, Mansfield SD, Campbell MM (2005) Light, the circadian clock, and sugar perception in the control of lignin biosynthesis. J Exp Bot **56:** 1651–1663

Rohde A, Morreel K, Ralph J, Goeminne G, Hostyn V, De Rycke R, Kushnir S, Van Doorsselaere J, Joseleau JP, Vuylsteke M, et al (2004) Molecular phenotyping of the pal1 and pal2 mutants of *Arabidopsis thaliana* reveals far-reaching consequences on phenylpropanoid, amino acid, and carbohydrate metabolism. Plant Cell **16:** 2749–2771

Schoch G, Goepfert S, Morant M, Hehn A, Meyer D, Ullmann P, Werck-Reichhart D (2001) CYP98A3 from *Arabidopsis thaliana* is a 3′-hydroxylase of phenolic esters, a missing link in the phenylpropanoid pathway. J Biol Chem **276:** 36566–36574

Schoof H, Zaccaria P, Gundlach H, Lemcke K, Rudd S, Kolesov G, Arnold R, Mewes HW, Mayer KF (2002) MIPS Arabidopsis thaliana database (MAtDB): an integrated biological knowledge resource based on the first complete plant genome. Nucleic Acids Res **30:** 91–93

Schumacher K, Vafeados D, McCarthy M, Sze H, Wilkins T, Chory J (1999) The Arabidopsis det3 mutant reveals a central role for the vacuolar H(+)-ATPase in plant growth and development. Genes Dev **13:** 3259–3270

Selvendran RR, March JF, Ring SG (1979) Determination of aldoses and uronic acid content of vegetable fiber. Anal Biochem **96:** 282–292

Sibout R, Eudes A, Pollet B, Goujon T, Mila I, Granier F, Seguin A, Lapierre C, Jouanin L (2003) Expression pattern of two paralogs encoding cinnamyl alcohol dehydrogenases in Arabidopsis: isolation and characterization of the corresponding mutants. Plant Physiol **132:** 848–860

Söderman E, Mattsson J, Engström P (1996) The Arabidopsis homeobox gene ATHB-7 is induced by water deficit and by abscisic acid. Plant J **10:** 375–381

Stafford H (1990) Flavonoid Metabolism. CRC Press, Boca Raton, FL

Stotz HU, Pittendrigh BR, Kroymann J, Weniger K, Fritsche J, Bauke A, Mitchell-Olds T (2000) Induced plant defense responses against chewing insects: Ethylene signaling reduces resistance of Arabidopsis against Egyptian cotton worm but not diamondback moth. Plant Physiol **124:** 1007–1018

Tamagnone L, Merida A, Stacey N, Plaskitt K, Parr A, Chang CF, Lynn D, Dow JM, Roberts K, Martin C (1998) Inhibition of phenolic acid metabolism results in precocious cell death and altered cell morphology in leaves of transgenic tobacco plants. Plant Cell **10:** 1801–1816

Tohge T, Nishiyama Y, Hirai MY, Yano M, Nakajima J, Awazuhara M, Inoue E, Takahashi H, Goodenowe DB, Kitayama M, et al (2005) Functional genomics by integrated analysis of metabolome and transcriptome of Arabidopsis plants over-expressing an MYB transcription factor. Plant J **42:** 218–235

Updegraff DM (1969) Semimicro determination of cellulose in biological materials. Anal Biochem **32:** 420–424

Vandepoele K, Raes J, de Veylder L, Rouzé P, Rombauts S, Inzé D (2002) Genome-wide analysis of core cell cycle genes in Arabidopsis. Plant Cell **14:** 903–916

Veit M, Pauli GF (1999) Major flavonoids from *Arabidopsis thaliana* leaves. J Nat Prod **62:** 1301–1303

Wasteneys GO (2004) Progress in understanding the role of microtubules in plant cells. Curr Opin Plant Biol **7:** 651–660

Weisshaar B, Jenkins GI (1998) Phenylpropanoid biosynthesis and its regulation. Curr Opin Plant Biol **1:** 251–257

Xiong L, Zhu JK (2003) Regulation of abscisic acid biosynthesis. Plant Physiol **133:** 29–36

Yamaguchi-Shinozaki K, Shinozaki K (1993) The plant hormone abscisic acid mediates the drought-induced expression but not the seed-specific expression of rd22, a gene responsive to dehydration stress in *Arabidopsis thaliana*. Mol Gen Genet **238:** 17–25

Yang YH, Dudoit S, Luu P, Lin DM, Peng V, Ngai J, Speed TP (2002) Normalization for cDNA microarray data: a robust composite method addressing single and multiple slide systematic variation. Nucleic Acids Res **30:** e15

Zhong R, Kays SJ, Schroeder BP, Ye ZH (2002) Mutation of a chitinase-like gene causes ectopic deposition of lignin, aberrant cell shapes, and overproduction of ethylene. Plant Cell **14:** 165–179

Downloaded from on May 22, 2019 - Published by www.plantphysiol.org
Copyright © 2006 American Society of Plant Biologists. All rights reserved.

CORRECTIONS

Vol. 140: 30–48, 2006

Abdulrazzak N., Pollet B., Ehlting J., Larsen K., Asnaghi C., Ronseau S., Proux C., Erhardt M., Seltzer V., Renou J.-P., Ullman P., Pauly M., Lapierre C., and Werck-Reichhart D. A *coumaroyl-ester-3-hydroxylase* Insertion Mutant Reveals the Existence of Nonredundant *meta*-Hydroxylation Pathways and Essential Roles for Phenolic Precursors in Cell Expansion and Plant Growth.

The authors regret that this article contains a description of immunofluorescence/confocal microscopy methodology that was not actually used for this work. In addition, this methodology was given without proper credit to Sugimoto et al. (K. Sugimoto, R.E. Williamson, G.O. Wasteneys [2000] Plant Physiol **124:** 1493–1506), who developed the protocol. The correct immunofluorescence/confocal microscopy methodology used for this article is described below. The authors apologize for this error and any inconvenience it may have caused.

Immunofluorescence Visualization of the Microtubules

Roots of 2-week-old seedlings were fixed in 2% (v/v) paraformaldehyde and 0.5% (v/v) glutaraldehyde in PEMT buffer (100 mM PIPES, 4 mM EGTA, 4 mM $MgSO_4$, 0.05% [v/v] Triton X-100, pH 7.2) for 40 min, and rinsed in PEMT buffer three times for 10 min. Roots were postfixed in cold methanol (−20°C) for 10 min on ice, rehydrated for 10 min in 1× PBS (136 mM NaCl, 2.7 mM KCl, 10 mM Na_2HPO_4, 2 mM KH_2PO_4, pH 7.4), and treated for 20 min with $NaBH_4$ (1 mg/mL) diluted in 1× PBS. Fixed roots were digested for 10 min with 0.2% (w/v) pectolyase, 1% (w/v) macerozyme, 3% (w/v) caylase diluted 10 times in digestion buffer (25 mM MES, 8 mM $CaCl_2$, 600 mM mannitol, pH 5.5). After three washes in PBSG buffer (1× PBS, 50 mM Gly), roots were incubated for 20 min in 5% normal goat serum diluted in PBSG to saturate nonspecific sites, then incubated with primary antibodies directed against α-tubulin (Molecular Probes) in PBSG at 4°C overnight and washed three times for 5 min in PBSG buffer. Samples were incubated for 1 h at room temperature with secondary antibodies coupled to Alexa Fluor 488 (Molecular Probes) and washed three times in PBSG buffer. Roots were mounted in Mowiol containing DABCO (100 mg/mL).

Observations were done using a Zeiss LSM510 confocal laser scanning microscope equipped with argon and helium/neon lasers and with a C-APOCHROMAT (× 63, 1.2 numerical aperture water immersion lens). Excitation/emission wavelengths were 488/bandpass 505 to 550 nm for Alexa 488. Image processing was done using LSM510 version 2.8 (Zeiss), ImageJ (W.S. Rasband; National Institutes of Health), and Photoshop 6.0 (Adobe Systems).

Vol. 141: 803–804, 2006

Plant Physiology regrets that the credit line was not included with the image of Pablo Picasso's *Woman with a Cigarette* in July's On the Inside feature. The Estate of Pablo Picasso has graciously granted permission to ASPB for use of this image in the print and online journal. The credit line for this image is as follows: © 2006 Estate of Pablo Picasso/Artists Rights Society (ARS), New York.

CORRECTIONS

Vol. 143: 924–940, 2007

Spencer M.W.B., Casson S.A., and Lindsey K. Transcriptional Profiling of the Arabidopsis Embryo.

On pages 927 and 928 of this article, the parenthetical citations for the supplemental figures are incorrect. Supplemental Figure S11A should be listed as Supplemental Figure 2A, Supplemental Figure 11B should be listed as Supplemental Figure 2B, and Supplemental Figure S12 should be listed as Supplemental Figure S3.

Vol. 140: 30–48, 2006

Abdulrazzak N., Pollet B., Ehlting J., Larsen K., Asnaghi C., Ronseau S., Proux C., Erhardt M., Seltzer V., Renou J.-P., Ullmann P., Pauly M., Lapierre C., and Werck-Reichhart D. A *coumaroyl-ester-3-hydroxylase* Insertion Mutant Reveals the Existence of Nonredundant *meta*-Hydroxylation Pathways and Essential Roles for Phenolic Precursors in Cell Expansion and Plant Growth.

In the title of this article, "*coumaroyl-ester-3′-hydroxylase*" was incorrectly printed as "*coumaroyl-ester-3-hydroxylase.*" Also, an incorrect manipulation in Figure 1 resulted in some double bonds missing in the published version. The corrected version of Figure 1 appears below.

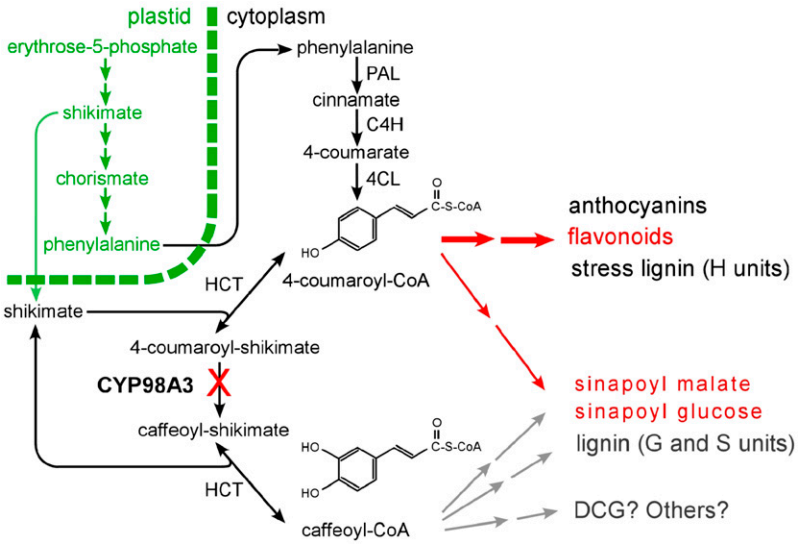

Figure 1. The phenylpropanoid pathway and modification occurring as a result of *CYP98A3* suppression. The pathways activated in the *cyp98A3* mutants are shown in red. The pathways inactivated are shown in gray. The monolignol DCG has been described as a growth regulator (Binns et al., 1987; Tamagnone et al., 1998). Aromatic amino acids, including Phe, are synthesized in the plastids via the so-called shikimate pathway (Herrmann and Weaver, 1999). The mode of transport of shikimate and Phe from the plastids to the cytoplasm is not yet described. 4CL, 4-Hydroxy cinnamoyl-CoA ligase.